NATIONAL ADVISORY COMMITTEE FOR AERONAUTICS

TECHNICAL NOTE 2297

EFFECT OF AN INCREASE IN ANGLE OF DEAD RISE ON THE HYDRODYNAMIC CHARACTERISTICS OF A HIGH-LENGTH-BEAM-RATIO HULL

By Walter E. Whitaker, Jr., and
Paul W. Bryce, Jr.

Langley Aeronautical Laboratory
Langley Field, Va.

Washington
February 1951

NATIONAL ADVISORY COMMITTEE FOR AERONAUTICS

TECHNICAL NOTE 2297

EFFECT OF AN INCREASE IN ANGLE OF DEAD RISE ON THE HYDRODYNAMIC CHARACTERISTICS OF A HIGH-LENGTH-BEAM-RATIO HULL

By Walter E. Whitaker, Jr., and
Paul W. Bryce, Jr.

SUMMARY

An investigation was made in Langley tank no. 1 to determine the effects of increasing the angle of dead rise on various hydrodynamic qualities of a flying-boat hull having a length-beam ratio of 15.

An increase in angle of dead rise from 20° to 40° increased the range of stable trim between the upper and lower trim limits of stability, increased the range of center-of-gravity position available for satisfactory take-off stability, and substantially improved the spray characteristics. The water resistance was increased appreciably in the planing range so that the take-off time and distance were increased approximately 25 percent and 30 percent, respectively. The over-all rough-water landing behavior was improved. The maximum vertical and angular accelerations were reduced approximately 55 and 30 percent, respectively.

INTRODUCTION

The development of high-speed water-based aircraft with the accompanying high wing loadings and stalling speeds has made the problem of hydrodynamic impact loads of increasing importance. Tank investigations of powered dynamic models have shown that appreciable reductions in accelerations are possible by increasing the hull length-beam ratio. An increase in hull length-beam ratio from 6 to 15 reduced the maximum vertical accelerations in waves approximately 25 percent without detriment to the other hydrodynamic qualities (references 1 and 2). These accelerations were further reduced by warping the forebody, by extending the afterbody, and by a combination of these hull modifications (references 3, 4, and 5, respectively).

Impact theory (reference 6), supported by experimental data (reference 7) on a prismatic float with no chine immersion, indicates an appreciable reduction in the hydrodynamic impact loads with increase in the angle of dead rise. The tank investigations on the hydrodynamic characteristics of hulls having a high length-beam ratio, therefore, were extended to include the effect of an increase in the angle of dead rise, not only on the rough-water accelerations and motions but also on the over-all hydrodynamic characteristics of a hull having a length-beam ratio of 15.

The model was the same as that used for the investigations described in references 1 and 2 with the exception of the basic angle of dead rise which was increased from 20° to 40°. The model was assumed to be a $\frac{1}{10}$-size powered dynamic model of a twin-engine, propeller-driven flying boat having a gross weight of 75,000 pounds, a gross-load coefficient of 5.88, a wing loading of 41.1 pounds per square foot, and a power loading for take-off of 11.5 pounds per brake horsepower. The hydrodynamic qualities determined in the investigation were longitudinal stability during take-off and landing, spray characteristics, take-off performance in smooth water, and the landing behavior in waves.

SYMBOLS

C_{Δ_o}	gross-load coefficient (Δ_o/wb^3)
Δ_o	gross load, pounds
b	maximum beam of hull, feet
g	acceleration due to gravity (32.2), feet per second^2
n_v	vertical acceleration, g units
α	angular acceleration, radians per second^2
w	specific weight of water (63.2 for these tests, usually taken as 64.0 for sea water), pounds per cubic foot
V	carriage speed (approx. 95 percent of airspeed), feet per second
V_v	sinking speed, feet per second
γ	flight-path angle, degrees

δ_e elevator deflection, degrees

τ trim (angle between forebody keel at step and horizontal), degrees

τ_L landing trim (trim at contact), degrees

T excess thrust (thrust available for acceleration), pounds

a longitudinal acceleration, feet per second^2

DESCRIPTION OF MODEL AND APPARATUS

The model (Langley tank model 266) used for this investigation was a modified version of Langley tank model 224 (reference 2), the modification being an increase in the basic angle of dead rise from 20° to 40° on both forebody and afterbody. Photographs and hull lines of the model are shown in figures 1 and 2. The general arrangement of the flying boat is shown in figure 3, and the offsets for the hull are presented in table I.

In deriving the hull having the 40° angle of dead rise, the plan form and profile (except for the chine line) were maintained identical to those of the basic hull with the 20° angle of dead rise. A constant angle of dead rise of 40° was maintained from the step (station 12) forward to station 7. From station 7 forward to the forward perpendicular, the angle of dead rise was uniformly increased so that at the forward perpendicular the angle of dead rise was the same as that of the basic forebody. (See fig. 4.) At each station between 2 and 12, the ratio of the flared chine height above the base line to that of the unflared chine height was the same as that of the basic forebody. The ratio varied slightly from station 2 to the forward perpendicular to give smooth fairing.

The investigation was conducted in Langley tank no. 1, which is described in reference 8. The apparatus used for the towing of dynamic models is described in reference 9. The setup of the model on the towing carriage is shown in figure 5. The model was free to trim about the pivot, which was located at the center of gravity and was free to move vertically but was restrained laterally and in roll and yaw. For the self-propelled-model tests in waves, the model had approximately 3 feet of fore-and-aft freedom with respect to the towing carriage in order to absorb the horizontal accelerations introduced by impacts. The longitudinal forces on the model were measured by use of a resistance dynamometer connected to the towing gear.

A strain-gage-type accelerometer mounted on the towing staff of the model measured the vertical accelerations. Two accelerometers of this type were used to measure the angular accelerations. These accelerometers, mounted 1 foot apart, were located within the model in such a manner that their centers of gravity were in line with the center of gravity of the model. In the static condition, all accelerometers read zero. The natural frequencies of the strain-gage accelerometers and the recording galvanometers used with the strain-gage accelerometers were about 180 and 40 cycles per second, respectively. The accelerometers were damped to approximately 0.7 of their critical values and the recording galvanometers to approximately 0.65 of their critical values. The frequency-response curve of the strain-gage-accelerometer and recording-galvanometer system was flat within ±5 percent between 0 and 21 cycles per second.

Slide-wire pickups were used to measure the trim, rise, and fore-and-aft position of the model. An electrically actuated trim brake attached to the towing staff fixed the trim of the model in the air during the landing approach. The trim brake was automatically released when the hull came in contact with the water. Electrical contacts were located at the sternpost, step, and at a point approximately 40 percent of the forebody length aft of the forward perpendicular in order to indicate when these parts of the model contacted the water. Wave struts, located forward and aft of the model and displaced laterally from the center line of the tank, were used to record the wave profiles and wave length. The apparatus for generating waves is described in reference 1.

PROCEDURE

A detailed description of the procedure followed in obtaining the hydrodynamic qualities covered in this investigation is presented in references 1 and 2. The hydrodynamic qualities determined include: trim limits of stability, the range of center-of-gravity position for satisfactory take-off stability, smooth-water landing stability, take-off performance, bow spray characteristics during take-off, tail spray characteristics during landings, and impact accelerations and landing behavior in rough water.

The hydrodynamic qualities were determined at a design gross load corresponding to 75,000 pounds, except for the spray investigation in which gross loads from 65,000 pounds to 95,000 pounds were included. The flaps were deflected 20° for all the hydrodynamic tests. Full thrust was used in determining the hydrodynamic qualities in all tests with the exception of the landing tests. The landings in smooth water

were made with approximately half thrust; whereas those in rough water were made with the thrust so adjusted that the model was self-propelled during most of the landing run. Landing and spray tests were made with the center of gravity at 32 percent mean aerodynamic chord. All data are presented as full-size values with the exception of the data in table II which are model values.

RESULTS AND DISCUSSION

Longitudinal Stability

Trim limits of stability.- The trim limits of stability for the hull having the 40° angle of dead rise are presented in figure 6 together with those for the basic hull having a 20° angle of dead rise. The lower limit for the hull with the 40° angle of dead rise was first encountered at a higher speed and lower trim than that for the hull with the 20° angle of dead rise. At planing speeds, the lower limit remained substantially the same. This behavior is not in agreement with the results reported in reference 10, which states that the lower trim limit should be raised by an increase in angle of dead rise. In the investigation described in reference 10, however, simple planing surfaces having dead-rise angles up to 30° and no chine flare, were used. Since unpublished data indicate that chine flare tends to lower the lower trim limit, the trend noted in figure 6 may be due to the greater effectiveness of the chine flare on the hull with the 40° angle of dead rise.

The upper trim limits (both upper and lower branches) were raised by the increase in angle of dead rise. This increase conforms to the trend reported in a previous investigation (reference 11) of the effect of angle of dead rise on high-angle porpoising characteristics of two simple planing surfaces in tandem. At trims and speeds corresponding to the upper trim limit, the wetted length on the forebody is small and the influence of possible differences in the effect of chine flare on this limit probably would be small. Agreement with results from tests of simple planing surfaces, therefore, might be expected.

Center-of-gravity limits of stability.- Typical trim tracks for the hull with 40° angle of dead rise covering a range of elevator deflection and center-of-gravity position are presented in figure 7(a). Comparable plots for the hull with the 20° angle of dead rise are shown in figure 7(b). The maximum amplitudes of porpoising during take-off were obtained from such data and have been plotted against center-of-gravity position in figure 8. The maximum amplitude of porpoising is defined as the difference between the maximum and

minimum trims during the greatest porpoising cycle that occurred during a take-off. Figure 8 shows only the forward limit since the maximum amplitude of upper-limit porpoising (after limit) never exceeded 1°.

The practical center-of-gravity limit for a given elevator deflection is usually defined as that position of the center of gravity at which the amplitude of porpoising becomes 2°. Such a limit has been determined from figure 8 and is shown as figure 9 together with the practical center-of-gravity limit for the hull with the 20° angle of dead rise. Increasing the angle of dead rise shifted the forward center-of-gravity limit forward over the entire range of elevator deflection and since there was no practical aft limit over the range of center-of-gravity position investigated, the stable range was substantially increased.

Landing stability.- Several typical time histories of smooth-water landings for the model with the 40° angle of dead rise are presented in figure 10(a). Comparable records for the basic hull with the 20° angle of dead rise are presented in figure 10(b). From such records the maximum and minimum values of trim and rise at the greatest cycle of oscillation were obtained and these data are plotted against trim at first contact in figure 11. The amplitude of oscillation in trim and rise was approximately the same for both hulls. No skipping tendency was obtained for the hull with the 40° angle of dead rise over a range of landing trim from 4° to 12°; therefore, it was concluded that the depth of step (16.5 percent beam) provided adequate ventilation.

Comparison of the records for both models indicates that the number of cycles necessary for the recovery from porpoising was less for the hull with 40° angle of dead rise. This reduction in number of cycles might be attributed to the increased damping effect caused by the deeper penetration of this hull.

Spray Characteristics

The spray characteristics of the hull with an angle of dead rise of 40° are presented in figures 12 to 15, along with comparative plots and photographs for the hull with an angle of dead rise of 20°. At design gross load, the hull with the 40° angle of dead rise had no heavy spray on the flaps and the speed range over which heavy propeller spray occurred was reduced. (See figs. 12, 13, and 14.) Photographs of the spray striking the horizontal-tail surfaces during a landing run are presented in figure 15. The forebody spray from both hulls struck the horizontal-tail surfaces at high speeds but the spray appeared to be less severe for the hull with the high dead-rise angle.

The increase in angle of dead rise resulted in a very definite over-all improvement in the spray characteristics. These improvements would be expected on the basis of results of a previous investigation of the effect of increase in angle of dead rise on a conventional hull (reference 12).

Take-Off Performance

The excess thrust and trim during take-off with full thrust for the hull with an angle of dead rise of 40° are shown in figure 16 together with a comparative plot for the hull with an angle of dead rise of 20°. The curves represent the excess thrust and trim for minimum total resistance except in the speed range where porpoising was encountered. Over this speed range the trim was increased above that for minimum resistance to avoid the lower trim limit of stability. Because of a change in the instrumentation for measuring horizontal forces, the excess thrust presented for the basic hull differs slightly from that recorded in reference 2.

Comparison of the excess thrust for both hulls indicates that the increase in angle of dead rise raised the water resistance over the entire take-off run. In the planing region, the excess thrust was reduced approximately 30 percent. The trim for minimum resistance remained approximately the same for both hulls throughout the take-off run with a maximum variation of less than 1° occurring at hump speed.

The longitudinal acceleration during take-off is plotted against speed in figure 17. The acceleration was derived from the excess-thrust curve in figure 16 by use of the relationship

$$a = \frac{Tg}{\Delta_o}$$

The take-off time was determined from the area under the curve of $1/a$ plotted against speed, and the take-off distance from the area under the curve of V/a plotted against speed. Increasing the angle of dead rise from 20° to 40° increased the take-off time and distance from 20 seconds and 1400 feet to 25 seconds and 1850 feet, or approximately 25 and 30 percent, respectively.

Rough-Water Landing Characteristics

Data obtained from records made during landings in waves are presented in table II. Information regarding the initial impact and the subsequent impacts which produced the maximum vertical and angular

accelerations with the corresponding trims at contact, sinking speeds, and flight-path angles is included in this table. The maximum accelerations are plotted against wave length in figures 18 and 19 together with the envelopes of similar data for the hull with an angle of dead rise of 20° (reference 1). The maximum accelerations usually occurred between the third and sixth impact.

The increase in angle of dead rise from 20° to 40° reduced the peak maximum vertical accelerations approximately 55 percent. In smooth water, the hydrodynamic impact loads for a prismatic float having an angle of dead rise of 40° (fig. 8 of reference 7) were approximately 50 percent lower than those for a hull having an angle of dead rise of 20°, and the experimental values were in good agreement with those predicted on the basis of impact theory (reference 6). In rough water, the hydrodynamic impact loads for prismatic floats also were in good agreement with the loads predicted on the basis of impact theory (reference 13). The effect of increase in angle of dead rise of the high-length-beam-ratio hull, therefore, was in good agreement with the effect expected on the basis of Langley impact basin experimental results and on the basis of impact theory. The effect of wave length on the vertical accelerations was not so pronounced with the hull having the high angle of dead rise as with the hull having the 20° angle of dead rise.

The maximum positive angular acceleration (bow rotated upward) of 8.7 radians per second per second, encountered by the hull with the 40° angle of dead rise, was approximately 30 percent less than the maximum positive angular acceleration encountered by the hull with the 20° angle of dead rise. Increase in the angle of dead rise had little effect on the maximum negative angular accelerations.

The maximum and minimum values of the trim and rise at the greatest cycle of oscillation during each landing in waves are plotted against wave length in figure 20. The increase in angle of dead rise had relatively little effect on the amplitude of trim oscillation at the greatest cycle. The maximum rise for the hull with a 40° angle of dead rise was reduced as compared with that for the hull with the 20° angle of dead rise. The minimum rise was increased slightly.

Summary Chart

A summary of the hydrodynamic qualities of a hull having a high angle of dead rise, as determined by the powered-dynamic-model tests, is presented in figure 21. This chart gives an over-all picture in terms of full-scale operational parameters and is therefore useful for comparisons with similar data regarding other seaplanes for which operating experience is available.

CONCLUSIONS

A comparison of the hydrodynamic qualities of a high-length-beam-ratio hull having an angle of dead rise of 40° with those for a similar hull having a 20° angle of dead rise indicates that the increase in angle of dead rise gave the following results:

1. The stable range of trim between the upper and lower trim limits of stability was increased over the entire speed range to take-off.

2. The forward center-of-gravity limit was moved forward and since there was no aft center-of-gravity limit, the stable range was substantially increased.

3. The smooth-water landing stability was approximately the same for both hulls. No skipping tendency was noted over the range of landing trim investigated.

4. The spray characteristics were substantially improved. At design gross load there was no heavy spray on the flaps and the speed range for heavy propeller spray was slightly reduced. The spray on the tail surfaces was slightly improved.

5. The water resistance was increased appreciably in the planing range so that the take-off time and distance were increased approximately 25 and 30 percent, respectively.

6. The rough-water landing characteristics were greatly improved. The maximum vertical and angular accelerations were reduced approximately 55 and 30 percent, respectively.

Langley Aeronautical Laboratory
National Advisory Committee for Aeronautics
Langley Air Force Base, Va., November 9, 1950

REFERENCES

1. Carter, Arthur W.: Effect of Hull Length-Beam Ratio on the Hydrodynamic Characteristics of Flying Boats in Waves. NACA TN 1782, 1949.

2. Carter, Arthur W., and Haar, Marvin I.: Hydrodynamic Qualities of a Hypothetical Flying Boat with a Low-Drag Hull Having a Length-Beam Ratio of 15. NACA TN 1570, 1948.

3. Carter, Arthur W., and Weinstein, Irving: Effect of Forebody Warp on the Hydrodynamic Qualities of a Hypothetical Flying Boat Having a Hull Length-Beam Ratio of 15. NACA TN 1828, 1949.

4. Kapryan, Walter J., and Clement, Eugene P.: Effect of Increase in Afterbody Length on the Hydrodynamic Qualities of a Flying-Boat Hull of High Length-Beam Ratio. NACA TN 1853, 1949.

5. Kapryan, Walter J.: Effect of Forebody Warp and Increase in Afterbody Length on the Hydrodynamic Qualities of a Flying-Boat Hull of High Length-Beam Ratio. NACA TN 1980, 1949.

6. Milwitzky, Benjamin: A Generalized Theoretical and Experimental Investigation of the Motions and Hydrodynamic Loads Experienced by V-Bottom Seaplanes during Step-Landing Impacts. NACA TN 1516, 1948.

7. Edge, Philip M., Jr.: Hydrodynamic Impact Loads in Smooth Water for a Prismatic Float Having an Angle of Dead Rise of 40°. NACA TN 1775, 1949.

8. Truscott, Starr: The Enlarged N.A.C.A. Tank, and Some of Its Work. NACA TM 918, 1939.

9. Olson, Roland E., and Land, Norman S.: Methods Used in the NACA Tank for the Investigation of the Longitudinal-Stability Characteristics of Models of Flying Boats. NACA Rep. 753, 1943.

10. Benson, James M., and Lina, Lindsay J.: The Effect of Dead Rise upon the Low-Angle Type of Porpoising. NACA ARR, Oct. 1942.

11. Benson, James M., and Klein, Milton M.: The Effect of Dead Rise upon the High-Angle Porpoising Characteristics of Two Planing Surfaces in Tandem. NACA ARR 3F30, 1943.

12. Bell, Joe W., and Willis, John M., Jr.: The Effects of Angle of Dead Rise and Angle of Afterbody Keel on the Resistance of a Model of a Flying-Boat Hull. NACA ARR, Feb. 1943.

13. Miller, Robert W.: Hydrodynamic Impact Loads in Rough Water for a Prismatic Float Having an Angle of Dead Rise of 30°. NACA TN 1776, 1948.

TABLE I

OFFSETS FOR LANGLEY TANK MODEL 266

[All dimensions are in inches]

Forebody														
Station	Distance to F.P.	Keel above base line	Chine above base line	Half-beam at chine	Angle of chine flare (deg)	Forebody bottom, height above base line								
						Buttocks								
						0.36	0.71	1.07	1.42	1.78	2.13	2.49	2.85	3.20
F.P.	0	10.30	10.30	0										
1/2	2.52	5.49	8.09	1.64	10	6.36	7.21	7.85	8.10					
1	5.04	3.76	6.75	2.18	10	4.49	5.23	5.96	6.52	6.73	6.76			
2	10.08	1.83	5.05	2.75	10	2.45	3.07	3.67	4.28	4.81	5.01	5.07		
3	15.12	.80	3.96	3.07	10	1.31	1.85	2.36	2.88	3.40	3.78	3.95	3.99	
4	20.15	.27	3.24	3.28	10	.73	1.18	1.63	2.09	2.55	2.92	3.16	3.26	3.25
5	25.19	.04	2.78	3.41	10	.43	.82	1.20	1.60	1.99	2.36	2.63	2.77	2.82
6	30.23	0	2.46	3.48	5	.33	.64	.97	1.29	1.62	1.94	2.22	2.39	2.47
7	35.27	0	2.30	3.50	0	.30	.60	.89	1.19	1.49	1.77	2.01	2.18	2.28
8	40.31	0	2.30	3.505	0	.30	.60	.89	1.19	1.49	1.77	2.01	2.18	2.28
9	45.34	0	2.30	3.505	0	.30	.60	.89	1.19	1.49	1.77	2.01	2.18	2.28
10	50.38	0	2.30	3.505	0	.30	.60	.89	1.19	1.49	1.77	2.01	2.18	2.28
11	55.42	0	2.30	3.505	0	.30	.60	.89	1.19	1.49	1.77	2.01	2.18	2.28
12F	60.51	0	2.30	3.505	0	.30	.60	.89	1.19	1.49	1.77	2.01	2.18	2.28

Afterbody				
Station	Distance to F.P.	Keel above base line	Half-beam at chine	Dead-rise angle (deg)
12A	60.51	1.16	3.505	40
13	65.50	1.63	3.45	40
14	70.54	2.11	3.31	40
15	75.58	2.58	3.10	40
16	80.61	3.06	2.85	40
17	85.65	3.54	2.48	40
18	90.69	4.01	2.04	40
19	95.73	4.49	1.46	40
20	100.77	4.97	.75	40
21	105.13	5.38	0	40

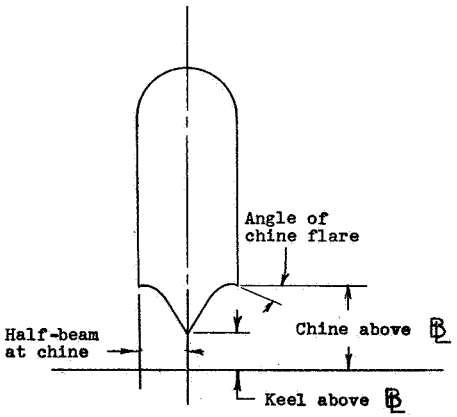

TABLE II

ROUGH-WATER LANDING DATA FOR LANGLEY TANK MODEL 266

[All values are model size;
wave height = 0.4 foot for all landings]

Landing	Wave length (ft)	τ_L (deg)	Initial impact						Maximum acceleration						
			τ (deg)	V_V (fps)	V (fps)	γ (deg)	n_V (g)	$\left(\frac{\text{radians}}{\text{sec}^2}\right)$[a]	Impact	τ (deg)	V_V (fps)	V (fps)	γ (deg)	n_V (g)	$\left(\frac{\text{radians}}{\text{sec}^2}\right)$[a]
1	15.3	7.6	7.6	1.17	39.4	1.7	1.3	4	5	4.9	1.66	33.3	2.8	2.2	40
									8	4.2	2.77	28.2	5.6	2.0	45
2	15.2	7.5	6.0	1.06	38.6	1.6	1.0	1	6	2.9	2.65	29.7	5.1	2.6	60
3	15.6	7.5	5.5	1.16	39.0	1.7	1.8	20	3	3.7	2.86	34.6	4.7	2.9	48
									5	3.3	2.63	31.8	4.7	2.7	62
4	15.9	7.6	7.5	1.33	36.0	2.1	1.1	0	5	4.0	2.76	30.9	5.1	2.7	62
5	15.9	7.5	6.1	1.09	38.8	1.6	1.0	5	5	4.1	3.13	31.0	5.8	3.3	65
6	15.3	7.5	6.9	1.06	39.0	1.5	1.0	0	5	4.0	2.04	33.1	3.5	2.5	50
7	15.7	7.5	6.0	1.14	38.8	1.7	1.3	15	3	4.0	3.04	34.1	5.1	3.0	50
									6	3.0	3.02	29.5	5.8	2.5	62
8	15.2	7.6	7.0	1.22	39.5	1.8	1.4	10	4	3.0	3.19	33.0	5.5	2.1	60
9	15.7	7.7	5.7	1.01	38.5	1.5	1.5	12	4	5.5	2.82	31.8	5.1	3.1	50
10	16.8	7.3	6.8	1.13	38.2	1.7	1.4	8	4	5.0	2.26	31.2	4.2	2.5	42
									5	2.5	3.43	29.3	6.7	2.5	60
11	16.8	7.3	6.4	1.11	37.0	1.6	1.2	7	3	3.1	4.02	32.3	7.1	3.9	83
12	16.4	7.5	6.3	1.15	39.8	1.6	1.4	8	5	5.0	3.39	31.0	6.2	3.9	64
13	16.8	7.6	6.8	1.23	39.2	1.8	1.6	10	6	2.9	3.45	30.4	6.5	2.9	88
14	17.3	7.5	7.5	.98	39.8	1.4	1.8	10	2	4.0	1.79	37.3	2.8	2.1	27
									3	3.7	1.91	35.9	3.0	1.9	29
15	17.2	7.7	6.2	1.12	40.0	1.6	1.4	10	5	4.3	2.70	33.0	4.7	2.9	47
									7	2.3	2.50	29.6	4.8	2.0	52
16	16.7	7.7	5.8	1.10	38.5	1.6	2.3	30	5	4.5	3.36	28.8	6.6	4.0	76
17	17.5	7.7	6.3	1.05	38.8	1.6	1.8	10	4	4.3	2.91	32.2	5.2	3.3	74
18	16.7	7.8	7.0	1.06	40.2	1.5	1.3	10	5	5.5	3.22	32.0	5.7	3.3	42
									4	3.6	2.91	36.0	4.6	3.0	60
19	16.6	7.9	7.3	1.30	40.5	1.8	1.5	12	5	5.6	3.16	33.0	5.5	3.6	60
									7	3.0	3.08	29.7	5.9	2.6	68
20	19.8	7.3	5.1	1.05	39.7	1.6	1.2	10	4	4.9	4.11	30.7	7.6	2.9	32
									3	3.7	4.04	33.1	7.0	2.7	48
21	19.6	7.3	6.5	1.14	36.8	1.7	1.4	9	4	4.2	3.52	31.3	6.4	3.7	55
22	19.0	7.3	7.3	1.08	39.4	1.6	1.2	0	7	3.8	4.03	30.5	7.5	2.4	52
23	19.7	7.3	5.2	.96	39.5	1.4	1.5	14	8	6.1	3.19	23.8	7.6	2.2	37
24	19.3	6.3	5.1	1.21	38.7	1.8	1.9	23	4	4.5	4.20	30.4	7.9	3.6	59
25	18.7	7.7	5.5	.99	38.0	1.5	1.5	9	3	4.0	3.60	33.0	6.2	4.2	63
26	19.7	7.7	5.0	1.03	38.9	1.5	2.0	21	4	4.1	3.84	30.9	7.1	3.7	46
27	19.8	9.3	5.0	1.03	38.7	1.5	1.9	21	4	4.3	3.70	30.7	6.9	4.0	60
28	19.8	8.4	5.5	1.14	40.3	1.6	2.0	21	5	5.5	3.90	32.5	6.8	3.9	49
29	19.5	8.2	8.2	1.05	40.0	1.5	1.4	7	3	5.5	3.83	35.0	6.2	3.2	46
30	22.7	7.5	4.5	1.07	39.3	1.5	1.9	21	2	6.9	3.07	36.2	4.8	3.0	43
31	22.2	7.4	5.2	1.03	38.0	1.5	1.2	8	4	3.8	3.64	31.5	6.6	3.0	46
32	22.8	7.4	7.4	1.15	38.8	1.7	1.2	0	6	5.4	3.51	27.7	7.2	2.2	32
33	22.2	7.4	5.9	1.12	38.8	1.6	1.4	16	2	4.0	3.11	35.8	5.0	2.2	38
34	22.1	7.5	7.5	1.14	38.7	1.7	.9	0	6	4.3	3.39	32.0	6.0	3.0	31
									5	3.2	2.35	34.2	3.9	2.0	39
35	23.1	7.5	5.9	1.08	38.0	1.6	1.4	12	4	3.4	3.83	30.2	7.2	3.2	53
36	23.1	7.5	6.0	1.11	38.0	1.7	1.4	16	4	3.4	4.41	30.0	8.4	3.3	59
37	22.3	7.7	5.0	.99	39.3	1.4	1.8	22	6	7.0	3.19	27.8	6.6	2.8	40
38	22.8	7.6	5.6	.92	39.0	1.3	1.1	8	3	4.2	2.54	34.6	4.2	2.3	30
39	22.4	7.6	7.6	1.11	38.4	1.6	1.2	5	5	4.6	3.83	32.1	6.8	3.0	50
40	22.6	7.3	5.4	1.08	37.9	1.6	1.1	9	7	6.6	2.85	25.5	6.4	1.9	27
41	23.3	7.6	5.3	1.14	36.2	1.7	.9	4	4	3.1	4.01	31.1	7.4	3.0	44
42	25.7	7.5	7.5	1.05	37.6	1.6	1.1	5	3	4.1	3.01	33.1	5.2	2.9	40
43	25.0	7.5	7.5	1.08	38.8	1.6	1.0	0	4	4.6	4.16	32.0	7.4	3.4	50
44	26.6	7.5	7.5	1.05	37.9	1.6	1.0	0	6	6.7	3.10	26.8	6.6	2.0	30
45	25.4	7.5	6.0	1.31	37.6	2.0	1.2	17	2	4.6	2.92	34.2	4.9	2.4	32
46	25.9	7.4	5.4	.98	37.2	1.5	1.5	20	3	4.8	4.29	31.7	7.7	2.6	30
47	26.0	7.4	4.9	.92	37.5	1.4	1.8	20	3	4.4	4.75	31.7	8.5	3.0	42
48	26.0	7.7	4.6	.92	39.4	1.3	1.2	19	3	3.6	3.89	33.2	6.7	2.8	45
49	25.8	7.7	5.6	1.02	38.4	1.5	1.0	10	7	6.9	3.04	26.8	6.5	2.1	20
50	26.1	7.7	7.7	1.03	39.2	1.5	1.0	2	3	4.0	3.64	34.5	6.0	2.7	40
51	25.5	7.7	5.1	1.10	38.9	1.6	1.4	20	3	3.6	3.76	32.8	6.5	3.0	50
52	32.5	7.6	7.6	1.06	38.9	1.6	1.0	5	3	4.2	3.88	33.5	6.6	2.7	40
									6	2.7	4.35	26.7	9.3	2.5	42
53	34.6	7.6	4.0	1.14	38.2	1.7	1.2	19	5	4.9	3.60	29.1	7.0	2.9	41
54	33.9	7.4	4.0	1.14	37.3	1.7	1.1	20	5	5.5	3.79	26.4	8.2	2.0	30
55	34.3	7.6	4.2	1.09	37.7	1.6	1.1	15	5	5.5	3.97	26.6	8.5	2.0	25
56	34.2	7.7	5.5	1.68	38.6	2.4	1.1	12	5	4.3	4.47	28.1	9.0	3.0	50
57	33.5	7.7	7.7	2.00	38.2	3.0	1.6	15	6	5.0	3.10	27.6	6.4	2.4	41
58	33.7	7.8	4.5	1.04	39.3	1.5	1.1	19	5	6.4	4.64	29.0	9.1	2.2	25
									6	5.5	3.23	27.0	6.8	2.0	28
59	32.6	7.7	7.7	1.02	39.9	1.4	1.1	6	3	5.0	3.80	34.2	6.4	3.2	40

[a]Impact for maximum angular acceleration.

NACA

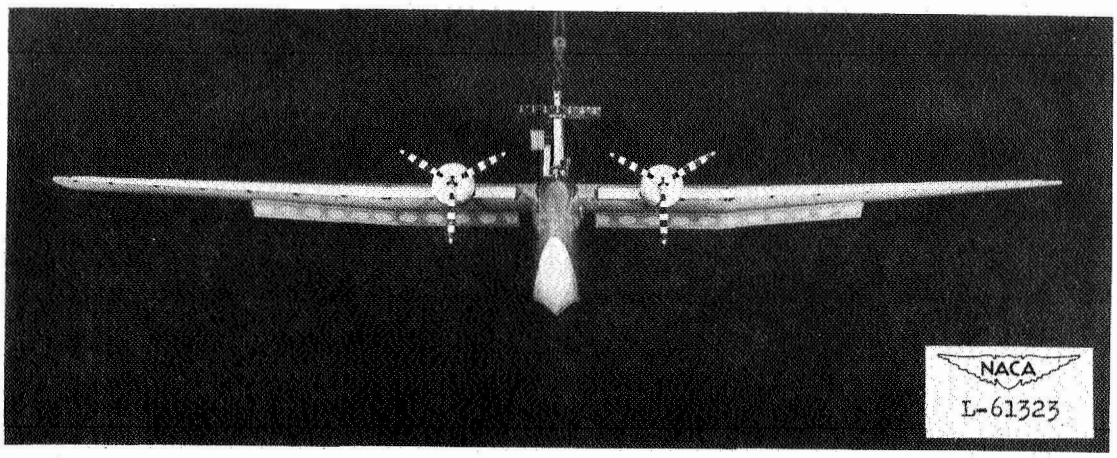

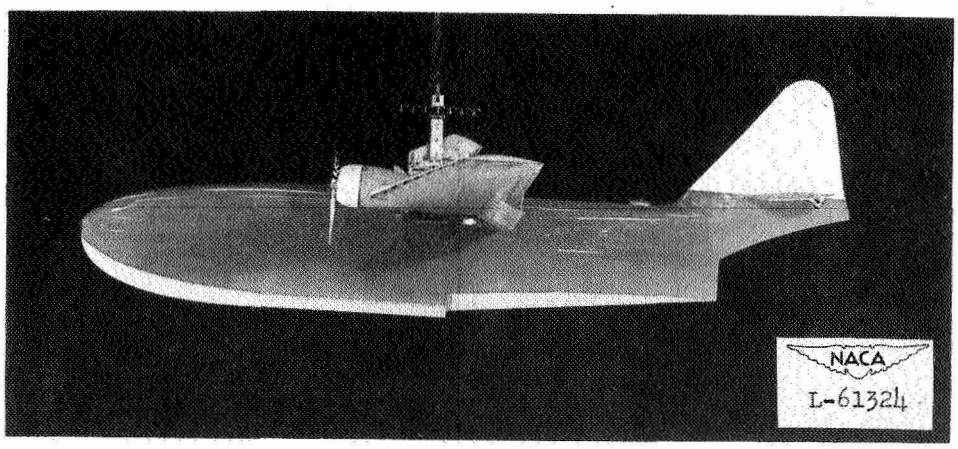

Figure 1.- Front and side views of Langley tank model 266.

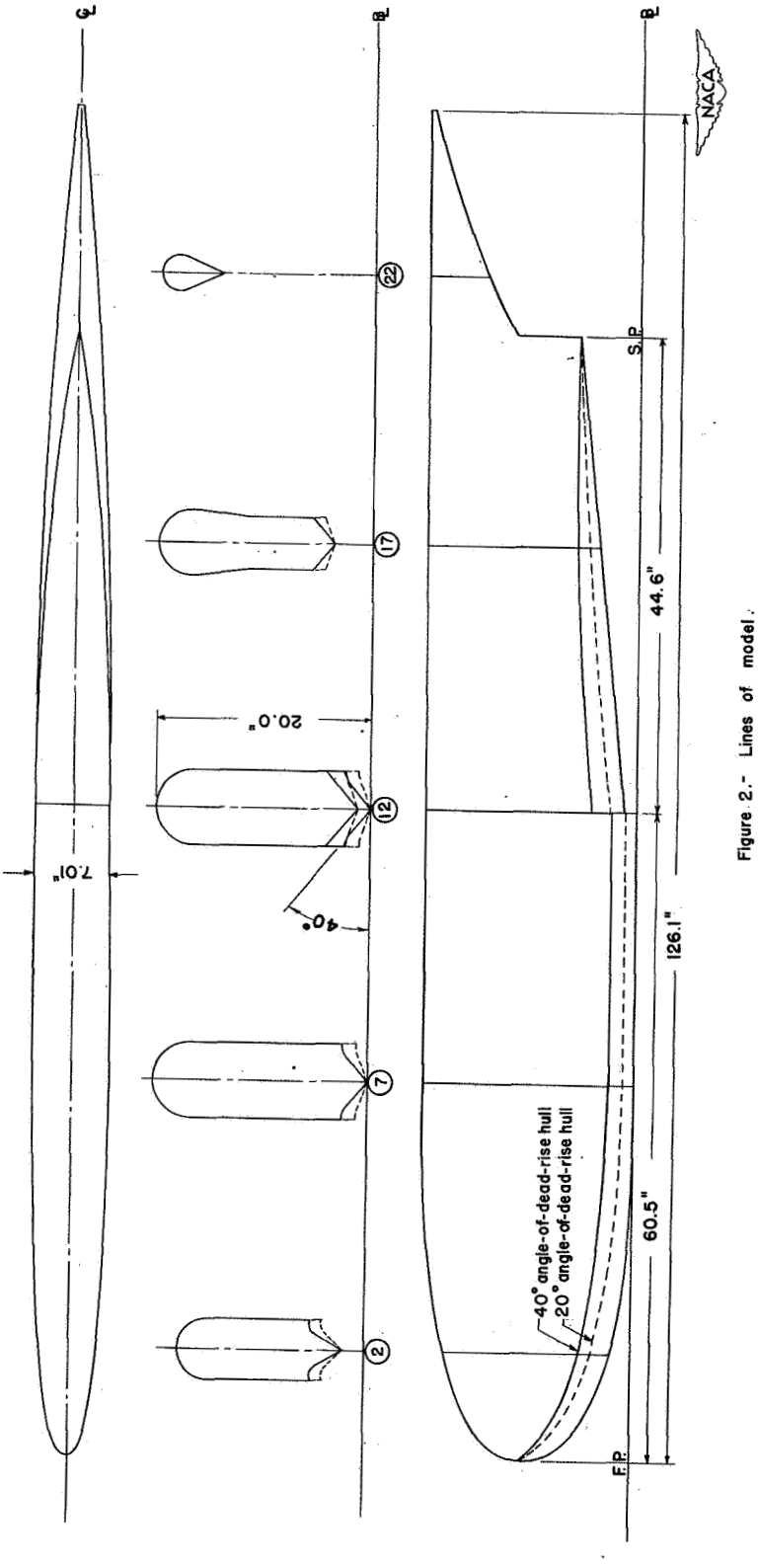

Figure 2.- Lines of model.

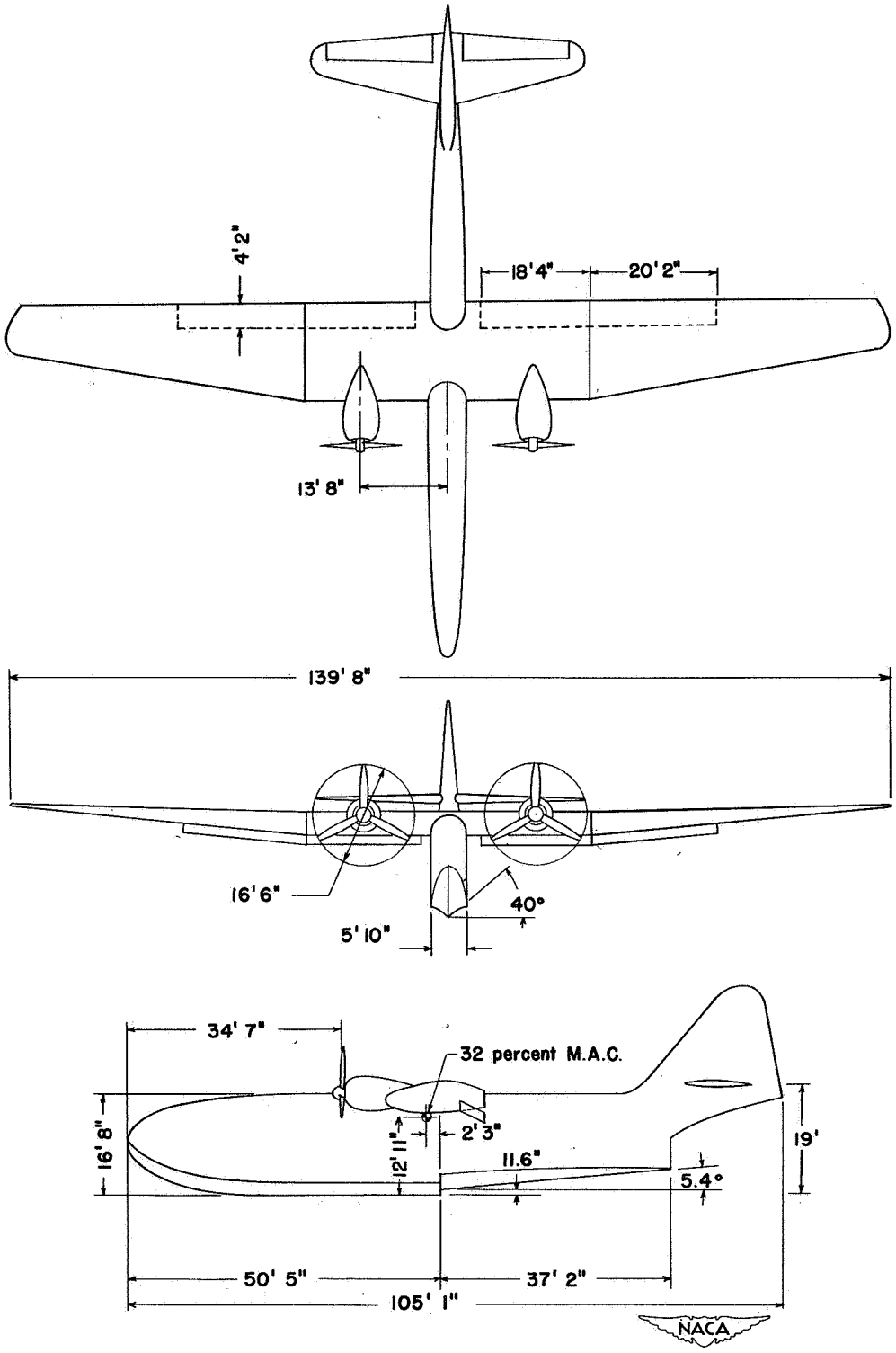

Figure 3.- General arrangement.

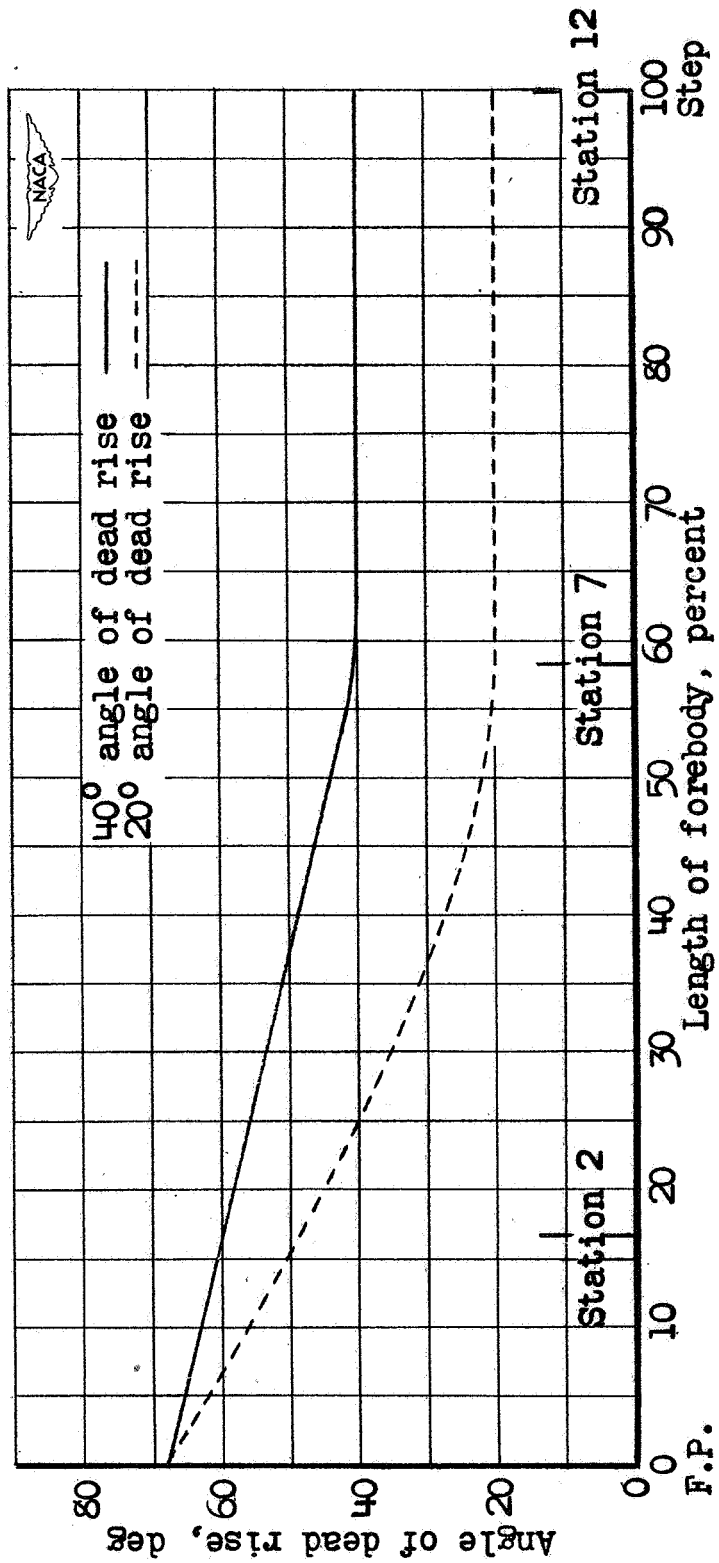

Figure 4.- Variation of basic angle of dead rise with length of forebody.

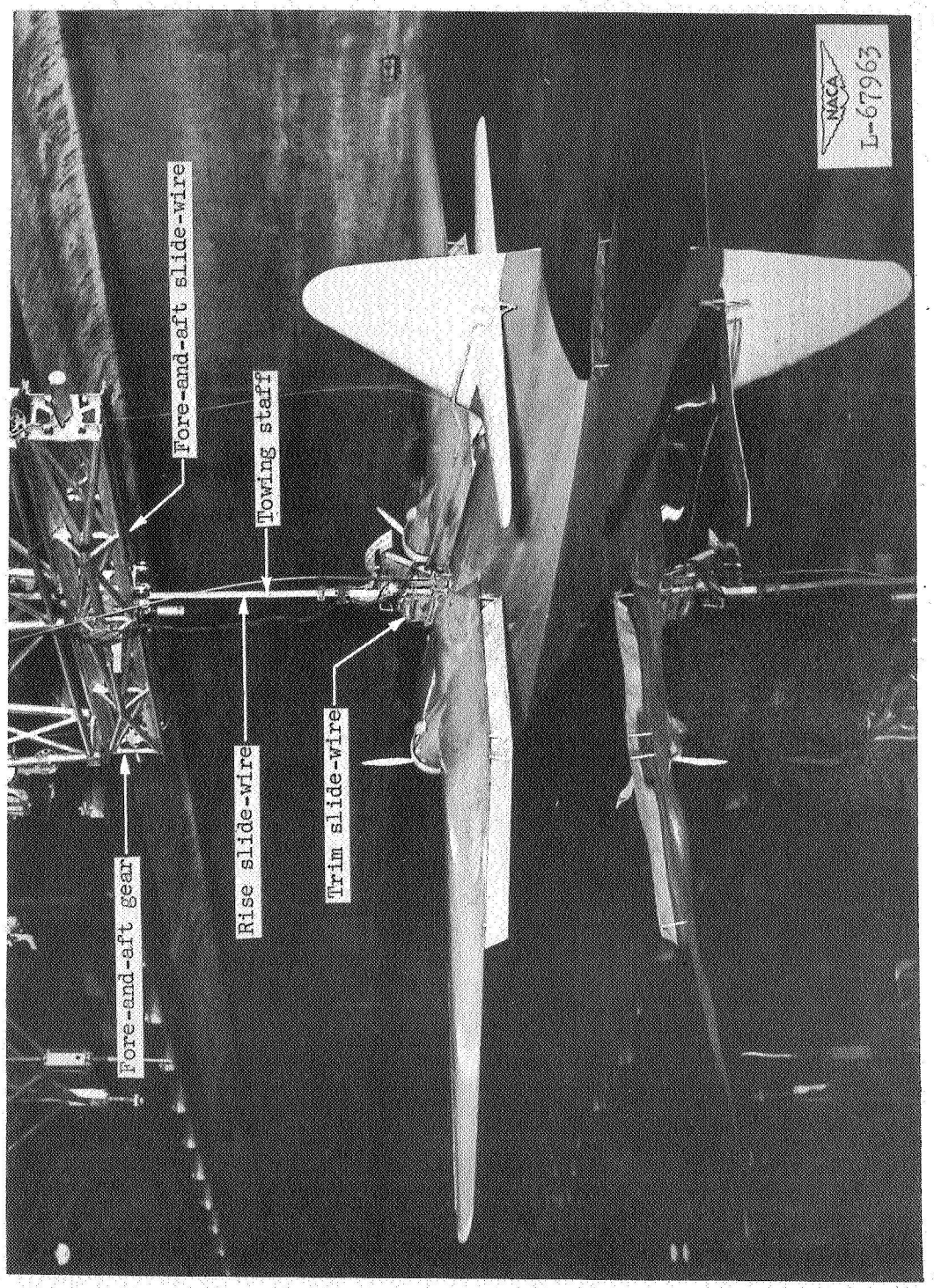

Figure 5.- Langley tank model 266 mounted on towing carriage.

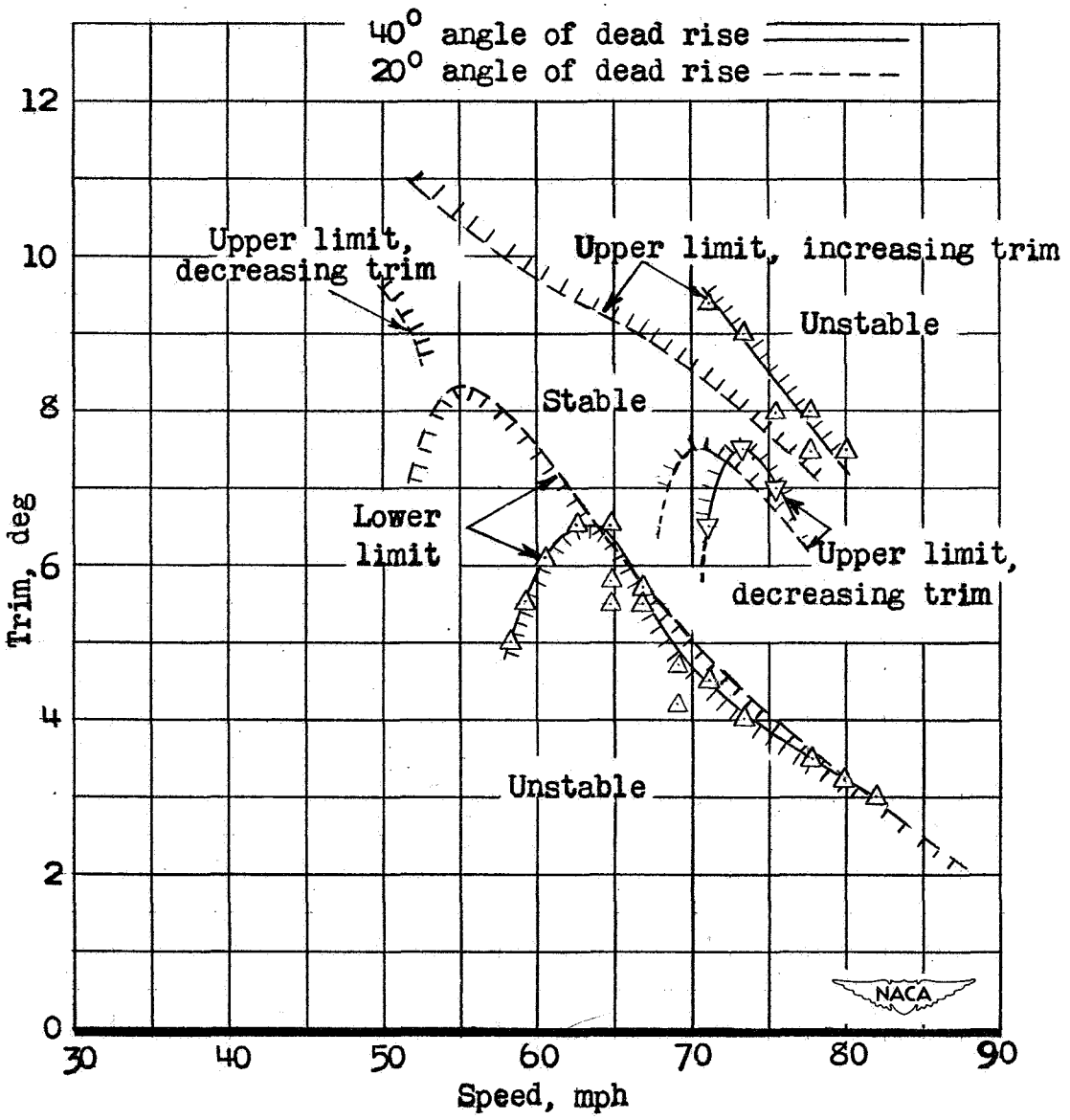

Figure 6.- Trim limits of stability.

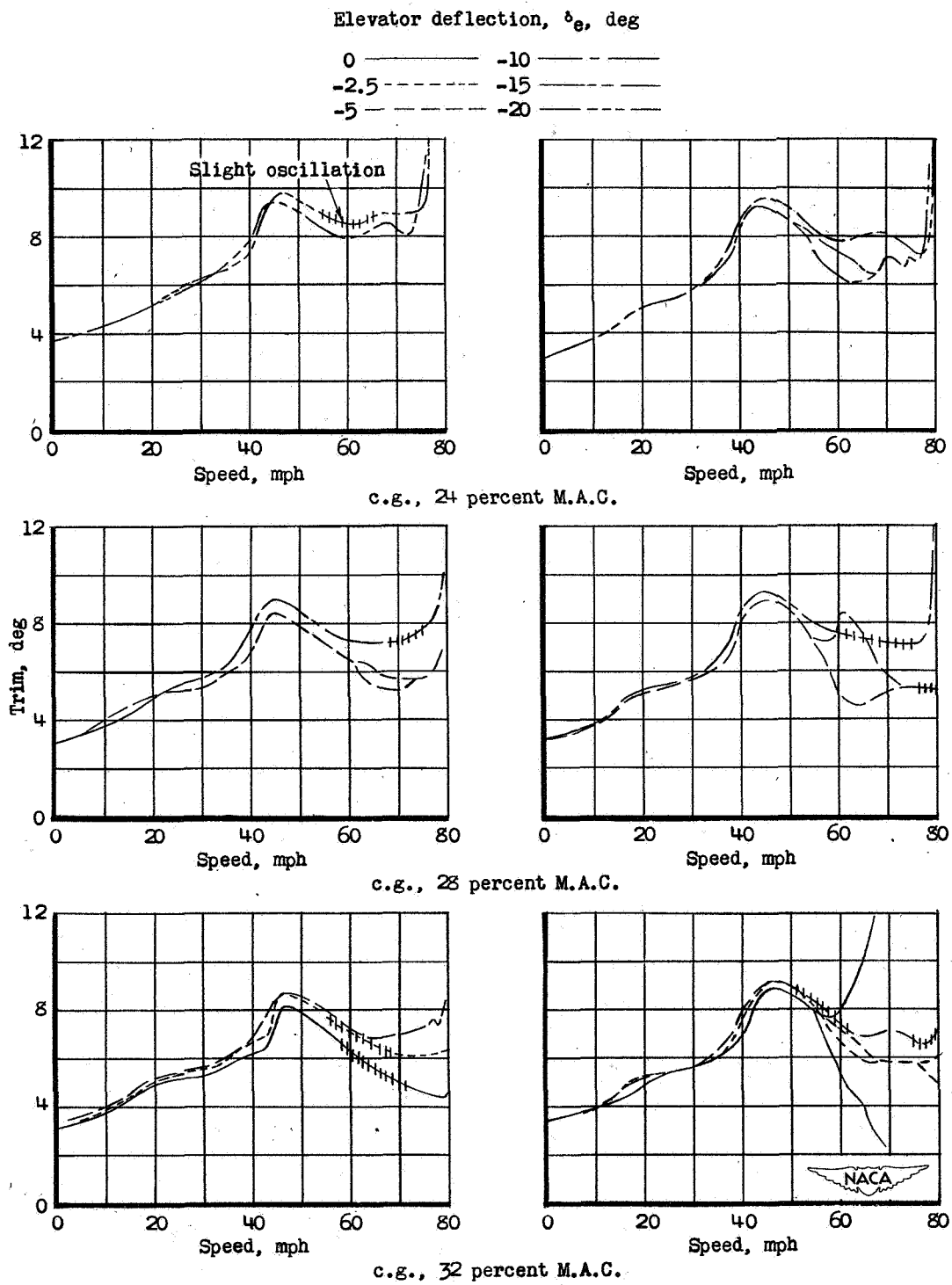

(a) 40° angle of dead rise. (b) 20° angle of dead rise.

Figure 7 .- Variation of trim with speed.

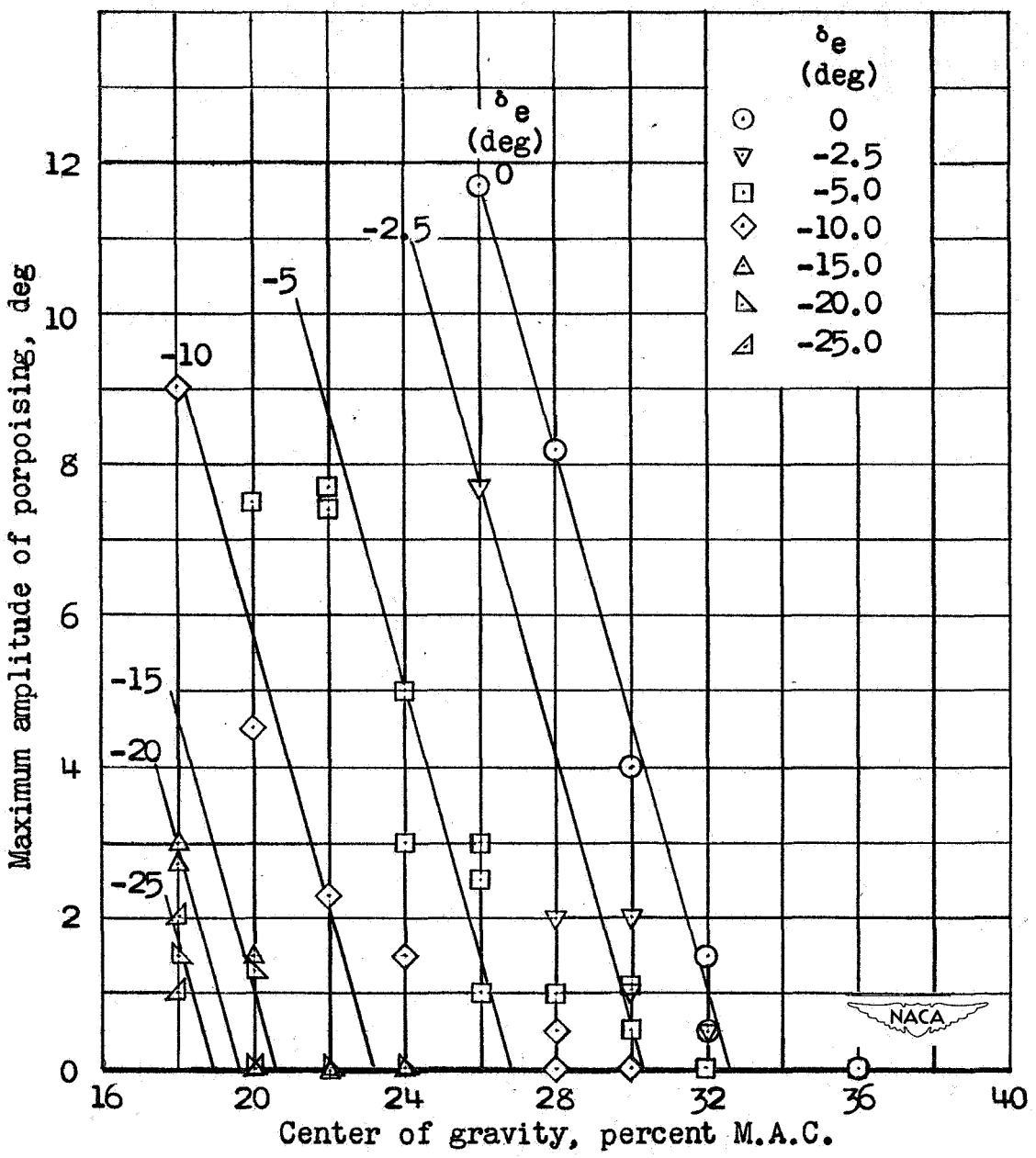

Figure 8.- Maximum amplitude of porpoising at different positions of the center of gravity; 40° angle of dead rise.

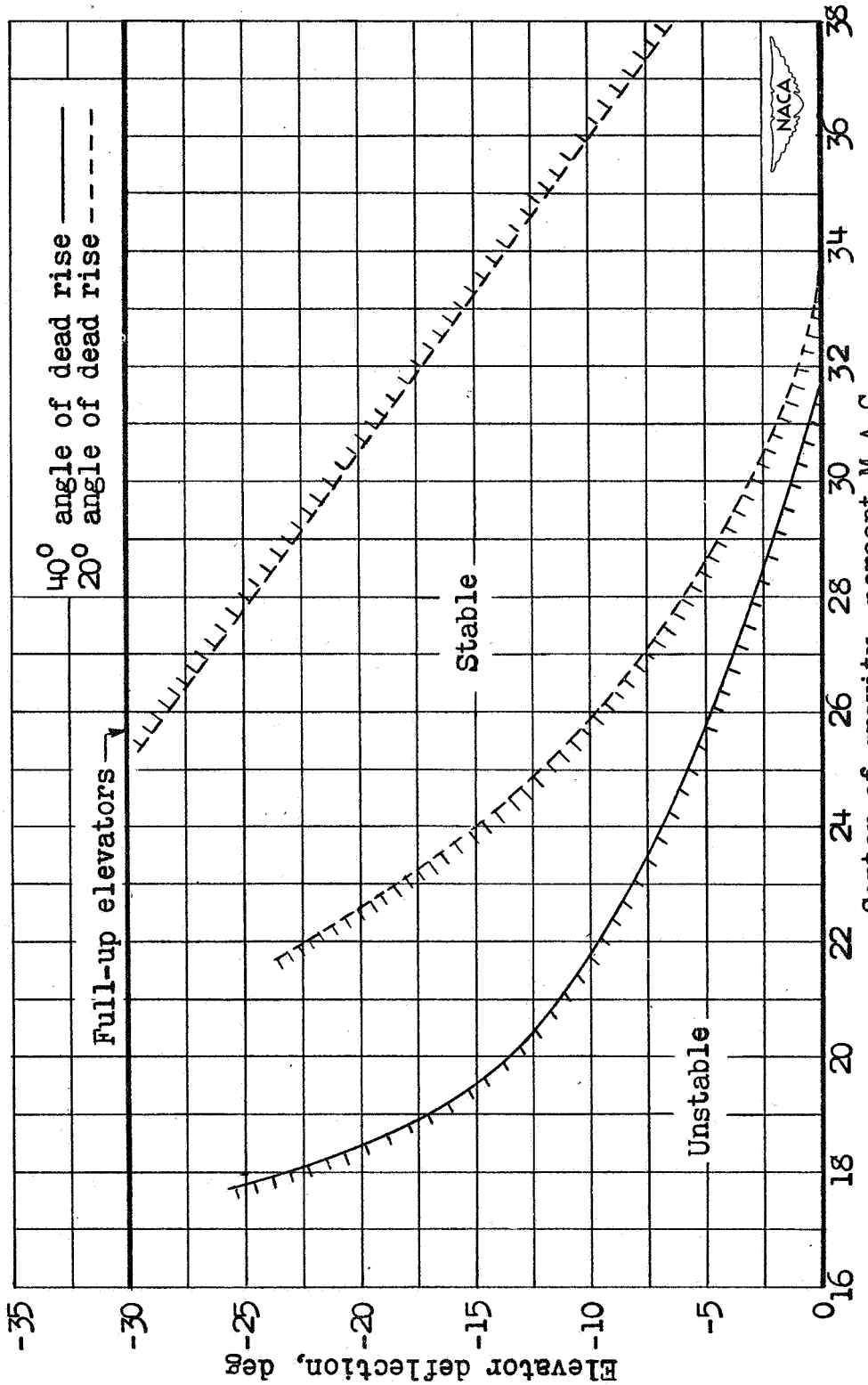

Figure 9 .- Center-of-gravity limits of stability for 2° amplitude of porpoising.

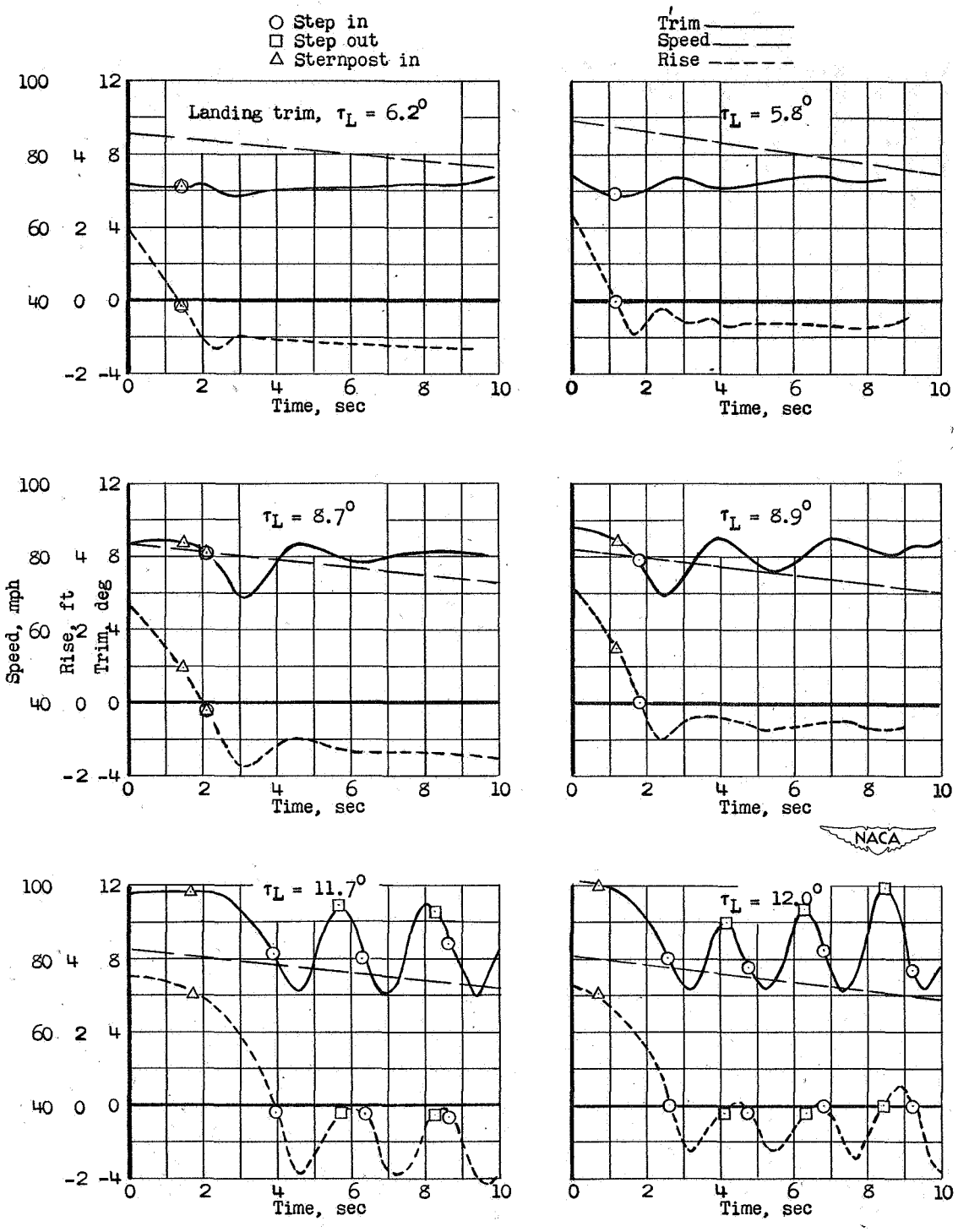

(a) 40° angle of dead rise. (b) 20° angle of dead rise.

Figure 10.- Variation of trim, rise, and speed with time during landings.

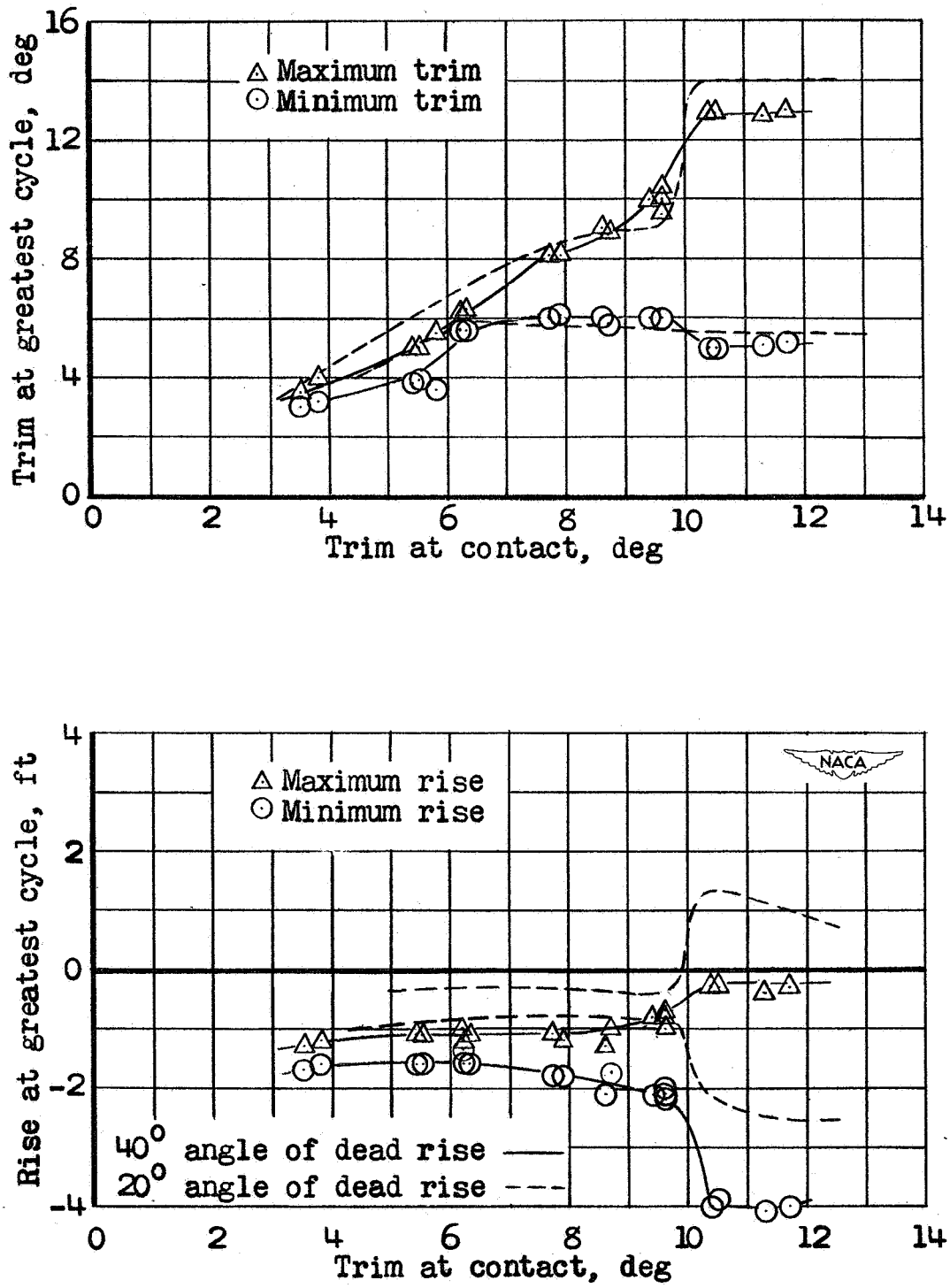

Figure 11.- Variation of maximum and minimum trim and rise with trim at contact.

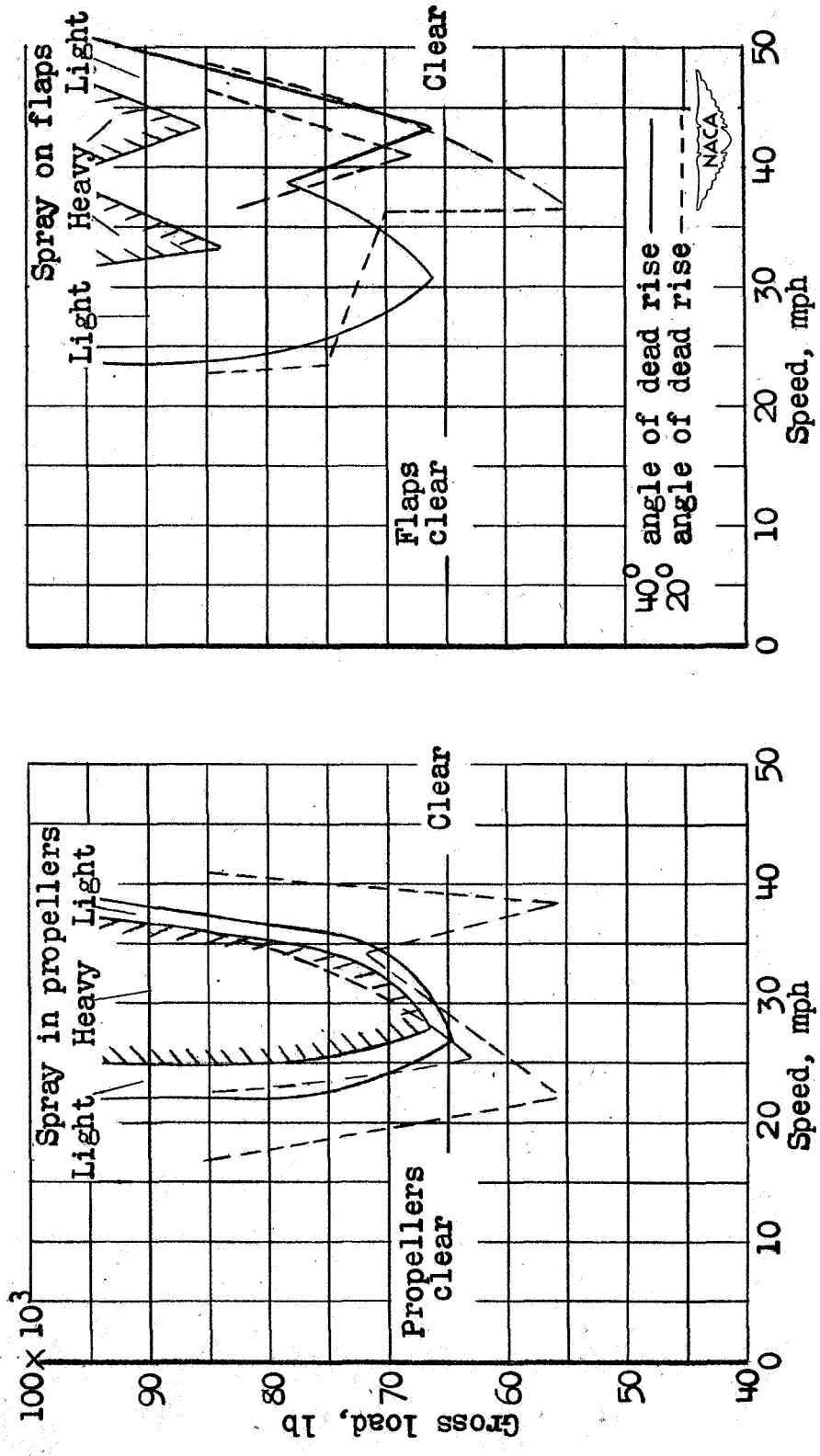

Figure 12.- Variation of range of speed for spray in propellers and flaps with gross load.

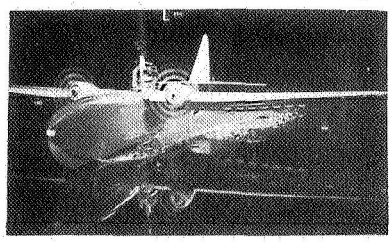

V = 25.9 mph; $\tau = 5.5^{\circ}$

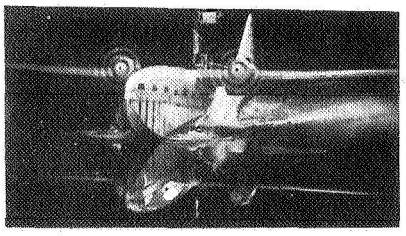

V = 23.7 mph; $\tau = 6.0^{\circ}$

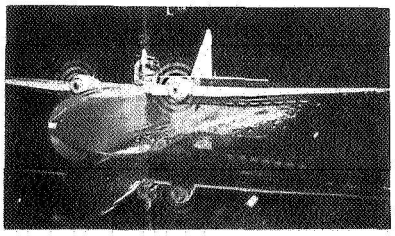

V = 28.0 mph; $\tau = 5.8^{\circ}$

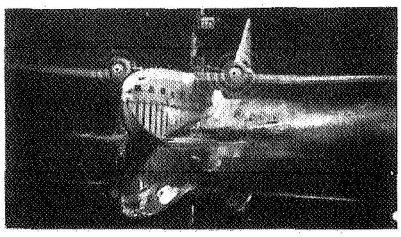

V = 25.9 mph; $\tau = 6.1^{\circ}$

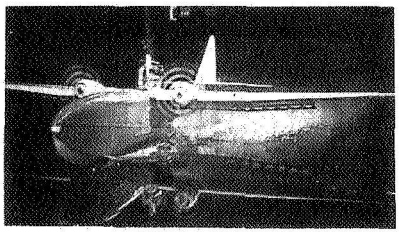

V = 30.2 mph; $\tau = 6.2^{\circ}$

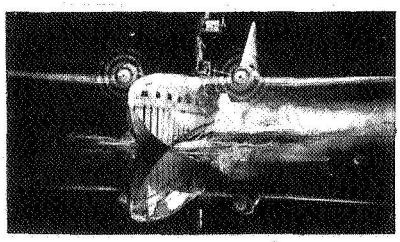

V = 28.0 mph; $\tau = 6.0^{\circ}$

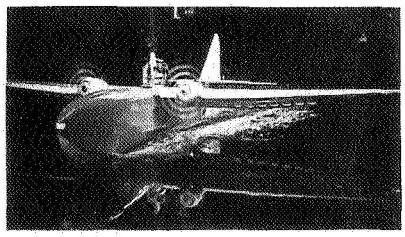

V = 32.3 mph; $\tau = 6.4^{\circ}$

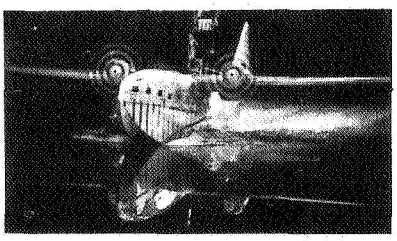

V = 30.2 mph; $\tau = 6.4^{\circ}$

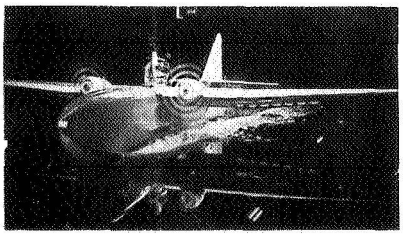

V = 34.4 mph; $\tau = 6.5^{\circ}$

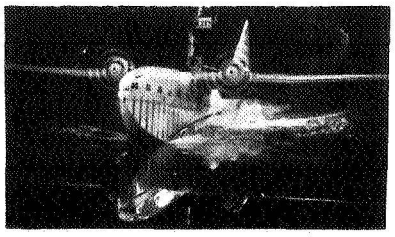

V = 32.3 mph; $\tau = 6.7^{\circ}$

(a) 40° angle of dead rise.

(b) 20° angle of dead rise.

NACA

L-67964

Figure 13.- Spray in propellers during take-off.

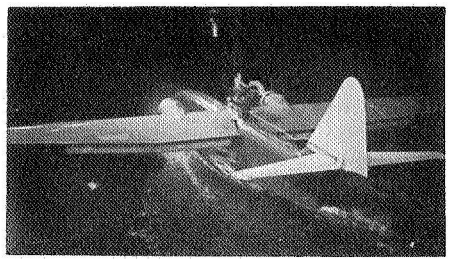

V = 25.9 mph; $\tau = 5.5^{\circ}$

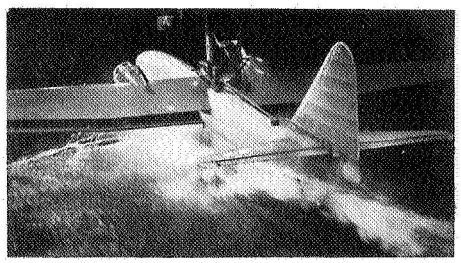

V = 38.8 mph; $\tau = 8.7^{\circ}$

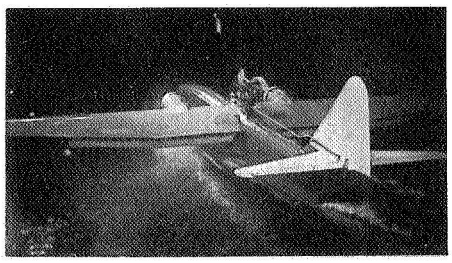

V = 30.2 mph; $\tau = 6.2^{\circ}$

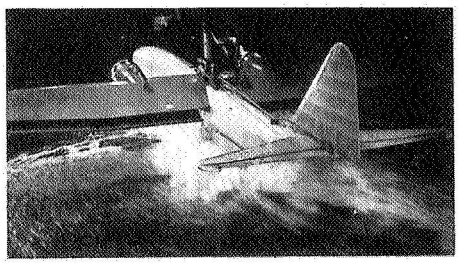

V = 41.0 mph; $\tau = 9.4^{\circ}$

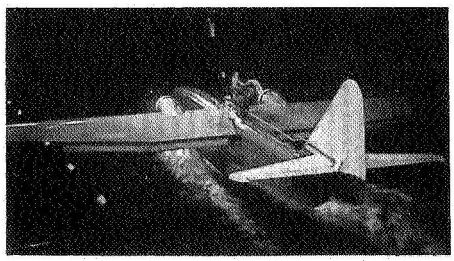

V = 34.4 mph; $\tau = 6.5^{\circ}$

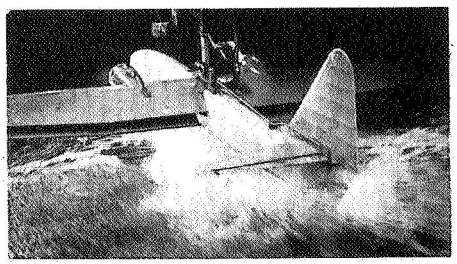

V = 43.1 mph; $\tau = 9.9^{\circ}$

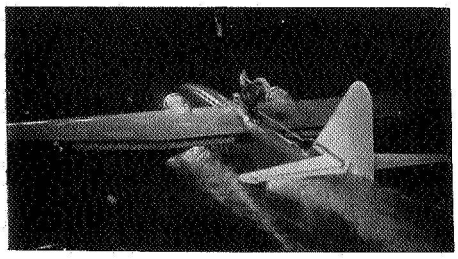

V = 38.8 mph; $\tau = 7.3^{\circ}$

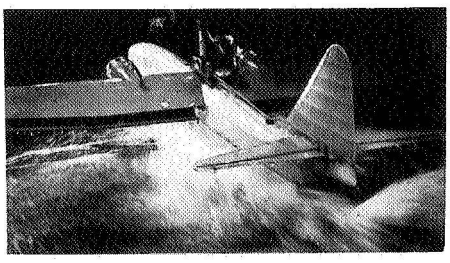

V = 45.3 mph; $\tau = 10.5^{\circ}$

NACA L-67965

(a) 40° angle of dead rise.

(b) 20° angle of dead rise.

Figure 14.- Spray on flaps during take-off.

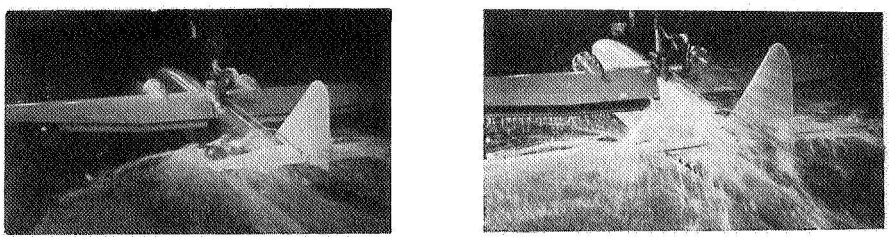

$\tau = 10.1^{\circ}$ V = 59.3 mph $\tau = 11.2^{\circ}$

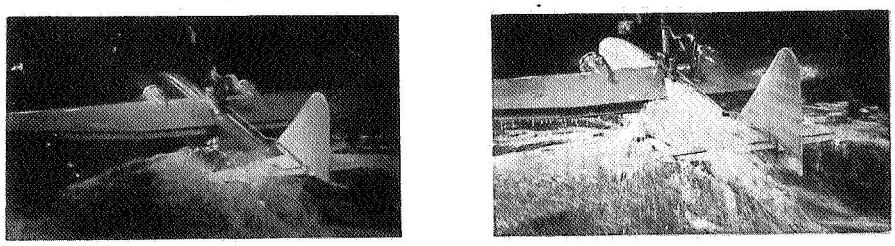

$\tau = 11.2^{\circ}$ V = 53.9 mph $\tau = 11.9^{\circ}$

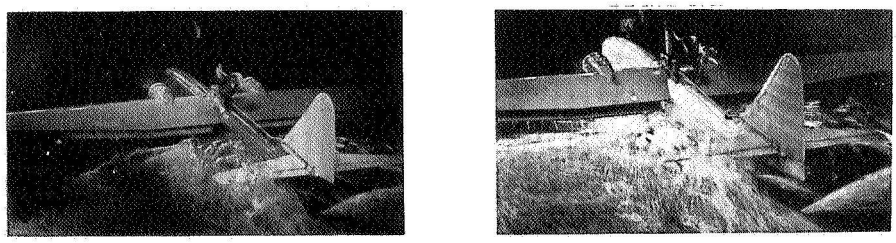

$\tau = 11.9^{\circ}$ V = 47.4 mph $\tau = 12.5^{\circ}$

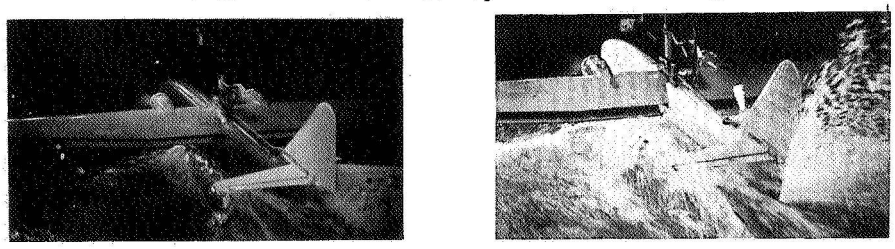

$\tau = 11.2^{\circ}$ V = 43.1 mph $\tau = 12.4^{\circ}$

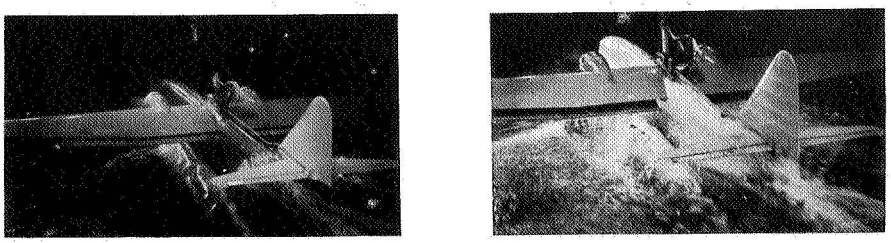

$\tau = 10.2^{\circ}$ V = 38.8 mph $\tau = 11.8^{\circ}$

NACA L-67966

(a) 40° angle of dead rise. (b) 20° angle of dead rise.

Figure 15.- Spray on tail surfaces during landing.

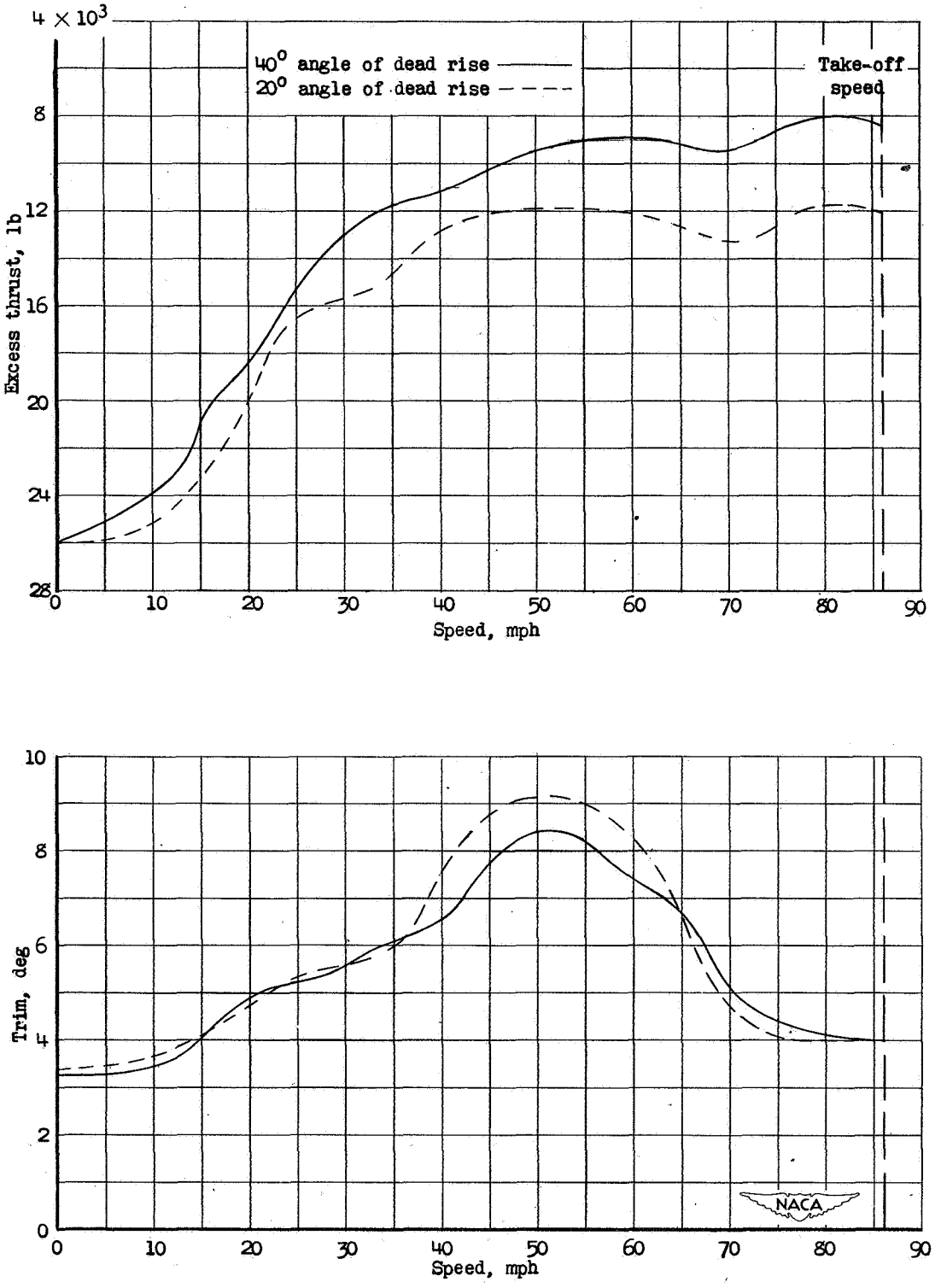

Figure 16.- Variation of excess thrust and trim with speed during take-off.

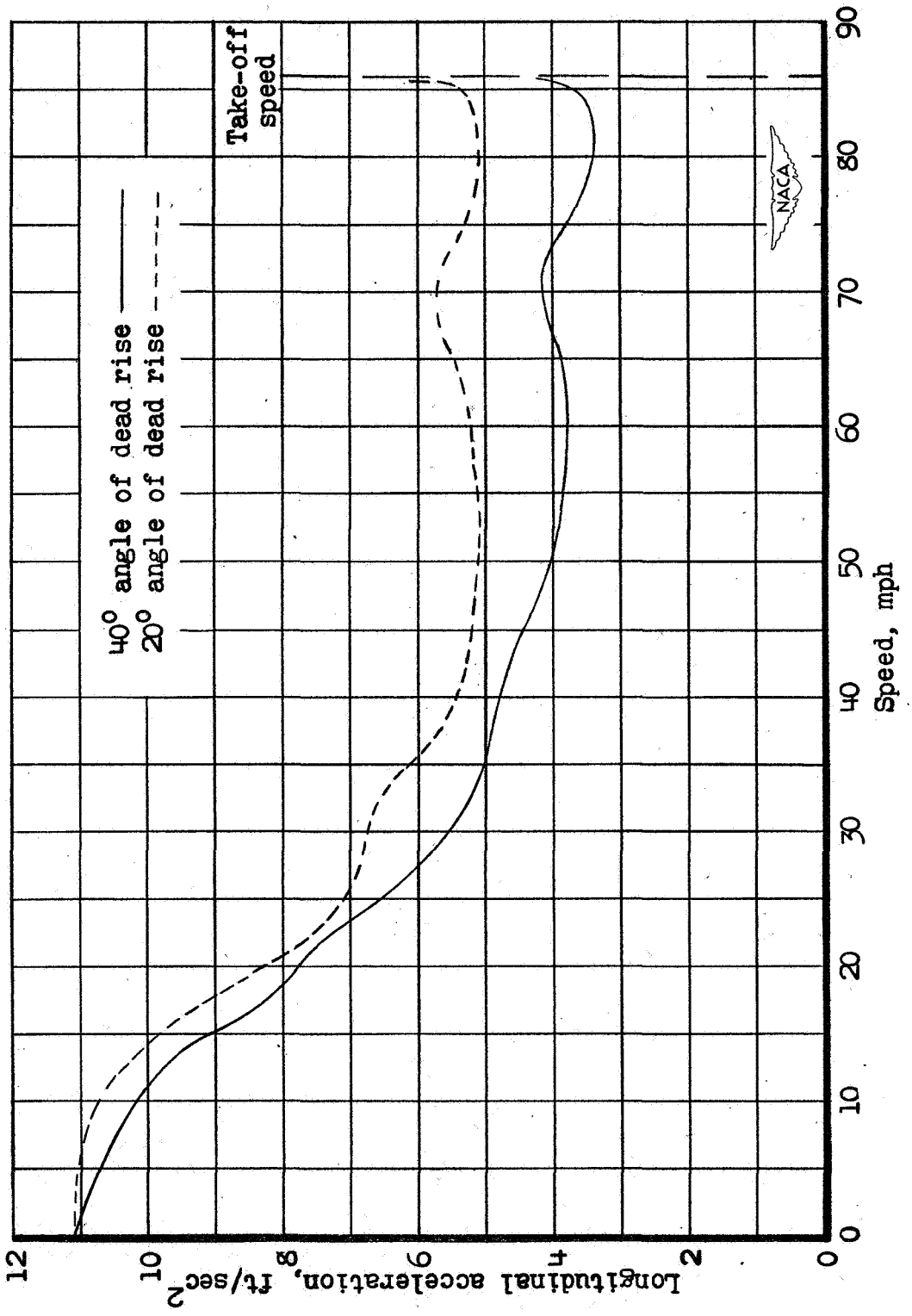

Figure 17.- Variation of longitudinal acceleration with speed during take-off.

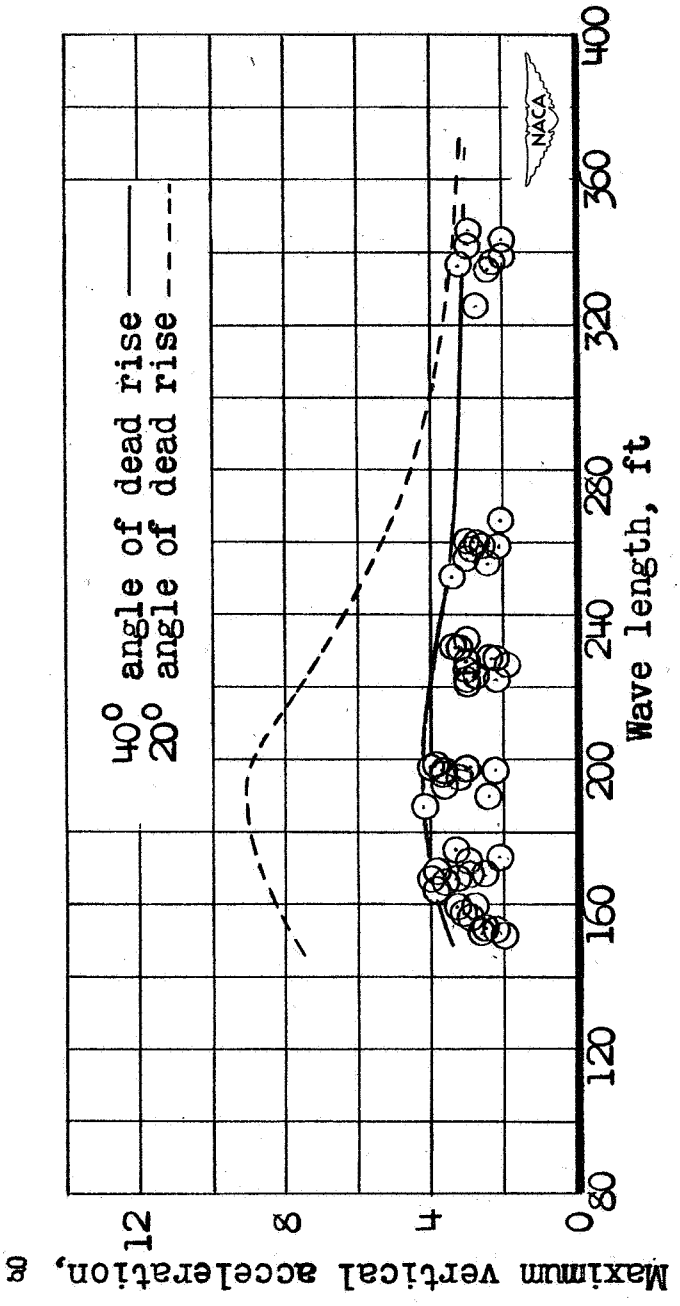

Figure 18.- Variation of maximum vertical acceleration with wave length. Wave height, 4 feet.

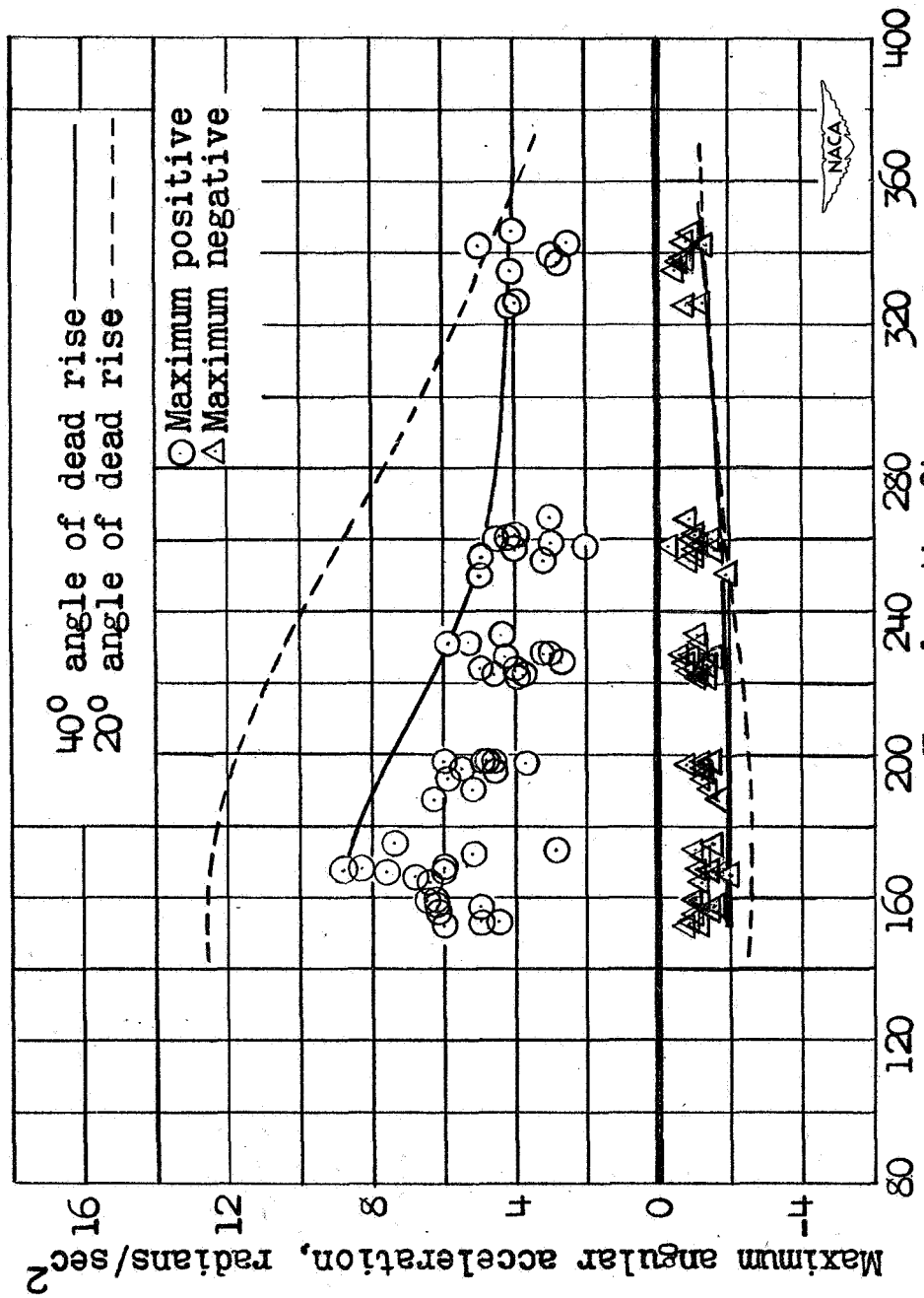

Figure 19.- Variation of maximum angular acceleration with wave length. Wave height, 4 feet.

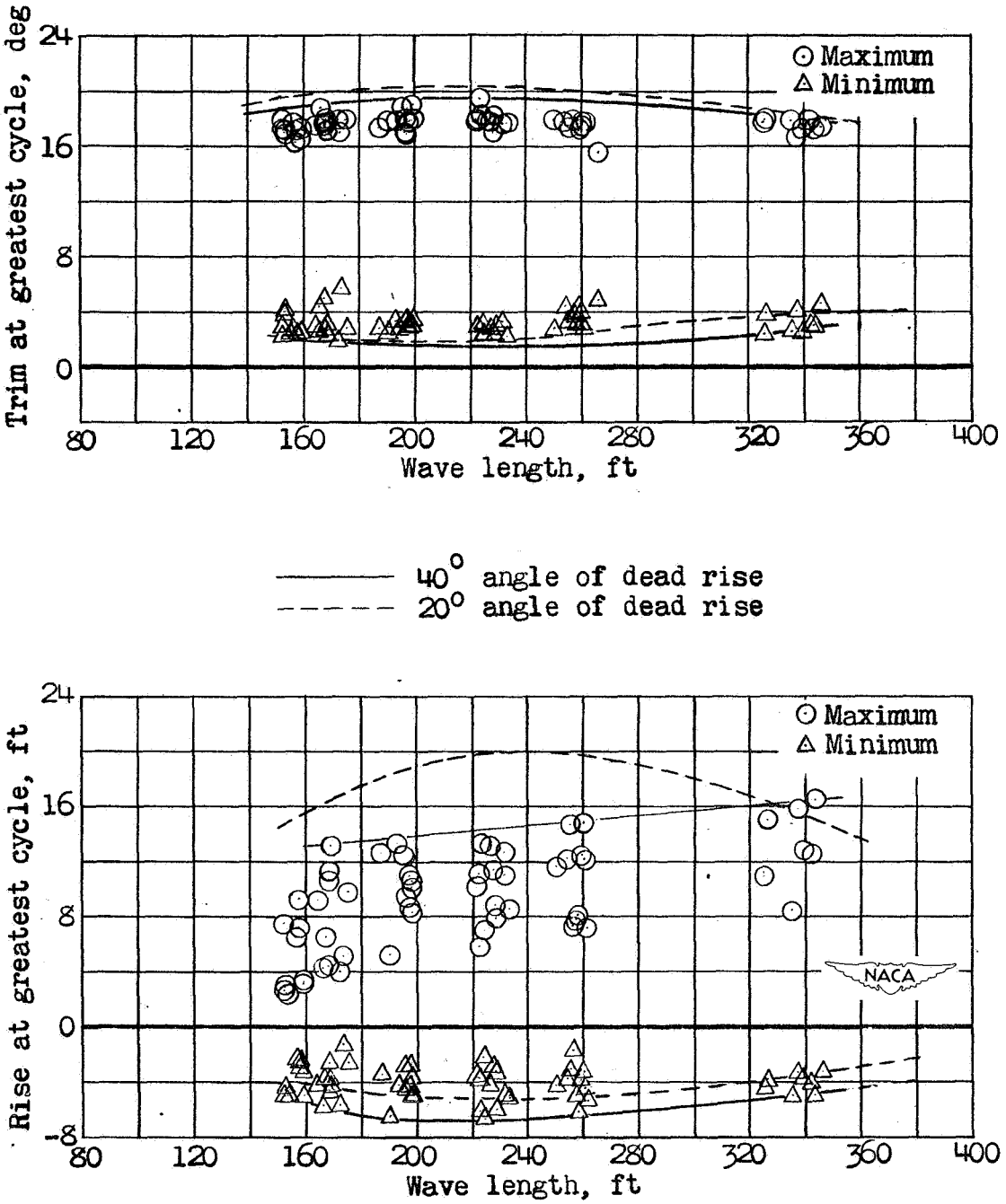

Figure 20.- Variation of maximum and minimum trim and rise with wave length. Wave height, 4 feet.

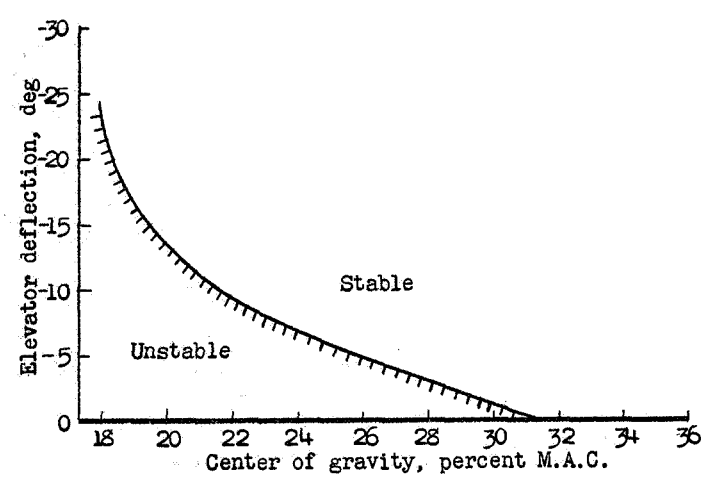

(a) Stable take-off range.

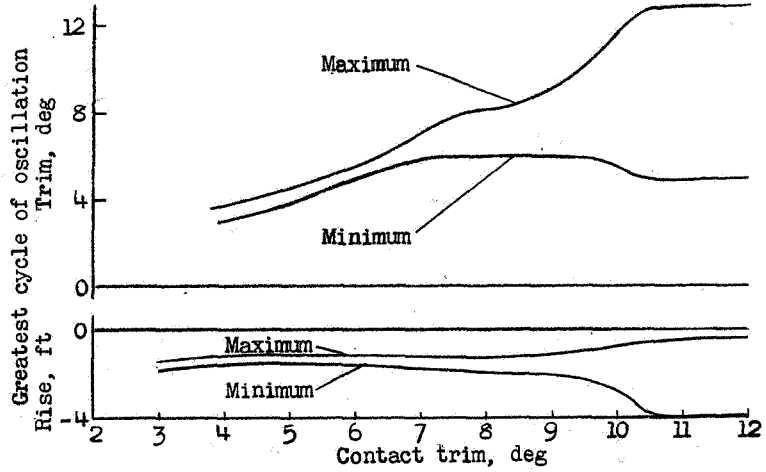

(b) Landing behavior in smooth water.

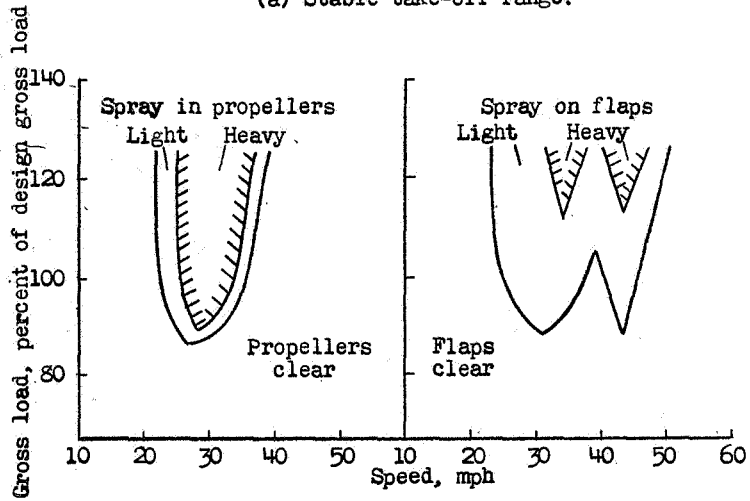

(c) Effect of gross load on spray.

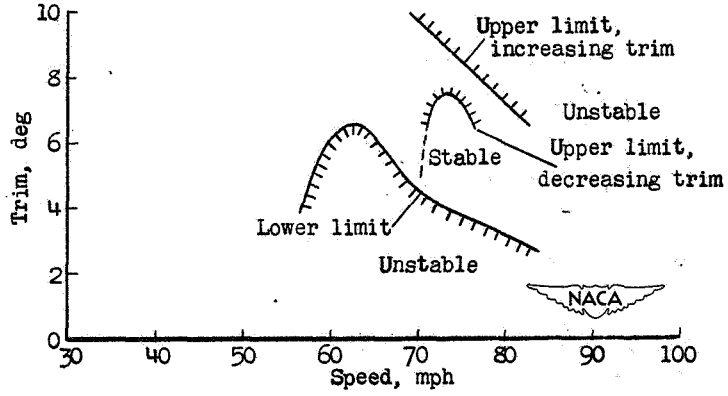

(d) Trim limits of stability.

Figure 21.- Summary chart of principal hydrodynamic qualities of a flying boat having a hull length-beam ratio of 15 with a 40° angle of dead rise. Gross load, 75,000 pounds; power loading, 11.5 pounds per brake horsepower; wing loading, 41.1 pounds per square foot; flap deflection, 20°.